Chemical Science

ROYAL SOCIETY OF CHEMISTRY

EDGE ARTICLE

View Article Online
View Journal | View Issue



Cite this: *Chem. Sci.*, 2025, **16**, 7347

All publication charges for this article have been paid for by the Royal Society of Chemistry



# Dinitrogen reduction to ammonia with a pincer-Mo complex: new insights into the mechanism of nitride-to-ammonia conversion†

Souvik Mandal,[a] Xiaoguang Zhou,[a] Quinton J. Bruch,[bc] Rachel N. Allen,[a] Laurence W. Giordano,[a] Nicholas J. I. Walker,[a] Thomas J. Emge,[a] Faraj Hasanayn,[d] Alexander J. M. Miller,[b] Santanu Malakar *[e] and Alan S. Goldman *[a]

The thioether–diphosphine pincer-ligated molybdenum complex (PSP)$MoCl_3$ (**1-Cl$_3$**, PSP = 4,5-bis(diisopropylphosphino)-2,7-di-*tert*-butyl-9,9-dimethyl-9*H*-thioxanthene) has been synthesized as a catalyst-precursor for $N_2$ reduction catalysis with a focus on an integrated experimental/computational mechanistic investigation. The (PSP)Mo unit is isoelectronic with the (PNP)Mo (PNP = 2,6-bis(di-*t*-butylphosphinomethyl)pyridine) fragment found in the family of catalysts for the reduction of $N_2$ to $NH_3$ first reported by Nishibayashi and co-workers. Electrochemical studies reveal that **1-Cl$_3$** is significantly more easily reduced than (PNP)$MoCl_3$ (with a potential *ca.* 0.4 eV less negative). The reaction of **1-Cl$_3$** with two reducing equivalents, under $N_2$ atmosphere and in the presence of iodide, affords the nitride complex (PSP)Mo(N)(I). This observation suggests that the $N_2$-bridged complex $[(PSP)Mo(I)]_2(N_2)$ is formed and undergoes rapid cleavage. DFT calculations predict the splitting barrier of this complex to be low, in accord with calculations of (PNP)Mo and a related (PPP)Mo complex reported by Merakeb *et al.* Conversion of the nitride ligand to $NH_3$ has been investigated in depth experimentally and computationally. Considering sequential addition of H atoms to the nitride through proton coupled electron-transfer or H-atom transfer, formation of the first N–H bond is thermodynamically relatively unfavorable. Experiment and theory, however, reveal that an N–H bond is readily formed by protonation of (PSP)Mo(N)(I) with lutidinium chloride, which is strongly promoted by coordination of $Cl^-$ to Mo. Other anions, *e.g.* triflate, can also act in this capacity although less effectively. These protonations, coupled with anion coordination, yield $Mo^{IV}$ imide complexes, thereby circumventing the difficult formation of the first N–H bond corresponding to a low BDFE and formation of the respective $Mo^{III}$ imide complexes. The remaining two N–H bonds required to produce ammonia are formed thermodynamically much more favorably than the first. Computations suggest that formation of the $Mo^{IV}$ imide is followed by a second protonation, then a rapid and favorable one-electron reduction, followed by a third protonation to afford coordinated ammonia. This comprehensive analysis of the elementary steps of ammonia synthesis provides guidance for future catalyst design.

Received 18th January 2025
Accepted 20th March 2025

DOI: 10.1039/d5sc00454c

rsc.li/chemical-science

## Introduction

The synthesis of ammonia from dinitrogen is perhaps the single most important industrially practiced chemical reaction, affording the fixed nitrogen for all synthetic fertilizer and thereby supporting approximately half of the world's food production.[1,2] The current dominant process, based on fossil fuel reforming and Haber–Bosch catalysis is responsible for nearly 2% of the world's fossil fuel consumption and $CO_2$ emissions.[1–4] There is thus great interest in the development of electrochemically driven nitrogen reduction.[5–18] Using a sustainable source of electrical energy, with water as the source of protons and electrons, such a process could in principle be essentially carbon-neutral. Such a process could also

[a]*Department of Chemistry and Chemical Biology, Rutgers, The State University of New Jersey, New Brunswick, New Jersey 08854, USA. E-mail: alan.goldman@rutgers.edu*
[b]*Department of Chemistry, University of North Carolina at Chapel Hill, Chapel Hill, North Carolina 27599, USA*
[c]*Department of Chemistry, Stony Brook University, Stony Brook, NY 11794, USA*
[d]*Department of Chemistry, American University of Beirut, Beirut 1107 2020, Lebanon*
[e]*Department of Chemistry, Rutgers University-Camden, Camden, New Jersey 08102, USA. E-mail: sm1792@chem.rutgers.edu*

† Electronic supplementary information (ESI) available: Complete experimental details and synthetic procedures, NMR data, computational details, computed energies and thermodynamic quantities. Optimized structures for calculated species. CCDC 2280371, 2329048 and 2340506–2340509. For ESI and crystallographic data in CIF or other electronic format see DOI: https://doi.org/10.1039/d5sc00454c

find applicability on a scale much larger even than the use of ammonia for fertilizer and chemicals, including the use of ammonia for storage and transportation of renewable energy or as a transportation fuel.[4,15,16]

In 2003 Schrock reported that a (triamidoamine)Mo complex (Fig. 1a) catalyzed the reduction and protonation of $N_2$ using $Cp^*_2Cr$ ($Cp^* = \eta^5$-$C_5Me_5$) as the source of electrons, and lutidine·$H^+$ ($LutH^+$) as the proton source.[19] This groundbreaking report represented the realization of a decades-old goal of a molecular catalyst for $N_2$ fixation; however, turnover numbers were quite low, selectivity for ammonia formation was low, and a very slow addition of reagents was required to achieve even these modest results. Nishibayashi subsequently reported[20,21] that the pincer-ligated dimeric Mo complex [(PNP)$Mo(N_2)_2]_2(\mu$-$N_2)$ (PNP = 2,6-bis(di-*t*-butylphosphinomethyl) pyridine) (Fig. 1b) catalyzed a similar reaction more efficiently, and later that the corresponding trihalides and nitridohalides were equally or more effective as catalyst precursors. Since then Nishibayashi and others have reported numerous other examples of pincer-ligated Mo catalysts, some of which yield extremely high turnovers, including systems that can utilize water as the proton source.[22–37] Most of these catalysts share the "PYP pincer" motif in which two terminal dialkyl- or diarylphosphino groups are connected to a neutral coordinating group such as the pyridine group of PNP, a central phosphino group, or an N-heterocyclic carbene group. Other Mo-pincer complexes have also been found to effectively catalyze ammonia formation or, in some cases, to effect the key $N_2$ cleavage step though not as part of a catalytic cycle for ammonia formation.[12,17,20–55]

These examples illustrate great progress in the development of molecular catalysts for $N_2$ fixation, and in particular they indicate the promise of pincer-Mo complexes as catalysts for $N_2$ reduction/protonation. Such complexes have very recently been found to be active catalysts for electrochemical reduction of $N_2$ to $NH_3$ as well, with[48] or without[54] a mediator. One of the challenges in the unmediated electrocatalysis is the need for highly negative applied potentials, which leads to competing $H_2$ evolution and presumably a high electrochemical overpotential; the development of a system with practical utility requires minimizing both of these factors.[11] Thus we have been particularly interested in designing new pincer Mo catalysts that are easier to reduce, while still maintaining good catalytic activity. More broadly, we have sought to expand the chemical space of (PYP)Mo-based catalysts while attempting to learn about the reaction mechanisms and the factors that govern the energetics of the numerous steps in any cycle catalyzed by such species. In this context, we report here the development of a (PSP)Mo-based system (PSP = 4,5-bis(diisopropylphosphino)-2,7-di-*tert*-butyl-9,9-dimethyl-9*H*-thioxanthene) for $N_2$ reduction, the observation of several catalytically relevant intermediates and their reactions, and a computational study of this chemistry with comparison to Nishibayashi's archetypal (PNP)Mo catalysts.[56]

The family of catalysts exemplified by (PNP)Mo is typically proposed to operate *via* cleavage of $N_2$ to give $Mo^{IV}$ nitrides which then undergo sequential "H atom additions" (*i.e.* PCET, either concerted or non-concerted) to the nitride ligand to give coordinated $NH_3$.[35–37,57,58] Importantly, the "first" (imide) N–H BDFE is generally much smaller than that of the second (amide) and third (ammonia); formation of the first N–H bond through PCET is thus relatively unfavorable and may lead to the highest barrier in the overall reaction.[35–37,57–61] The results presented herein, both experimental and computational, indicate that in fact this first N–H bond is not actually formed by PCET, but instead by protonation and addition of an anion, for both (PSP)Mo- and (PNP)Mo-based systems. This is then followed by PCET to the resulting $Mo^{IV}$ imide, to form an amide; the energetics of this step correlate with a BDFE that is similar to that for the conventionally proposed $Mo^{III}$ imide intermediate. The third and final N–H BDFE, corresponding to PCET to the resulting $Mo^{III}$ amide, is similar to that for the $Mo^{II}$ amide of the commonly proposed cycle. Thus, the formation of $NH_3$ from nitride is achieved by "circumventing" the energetically unfavorable step of PCET to the nitride intermediate.

## Experimental results and discussion

### Synthesis and characterization of (PSP)$MoCl_3$

The pincer ligand PSP was synthesized as we have reported previously.[62] Its reaction with $MoCl_3(THF)_3$ in THF solution gave **1-Cl$_3$** in good yield (**1** = (PSP)Mo; Scheme 1). The $^1$H NMR spectrum (THF-$d_8$) was consistent with a single, paramagnetic species. Crystals were obtained by diffusion of pentane into a THF solution, and the molecular structure was determined by single-crystal X-ray diffraction (scXRD) (Fig. 2).

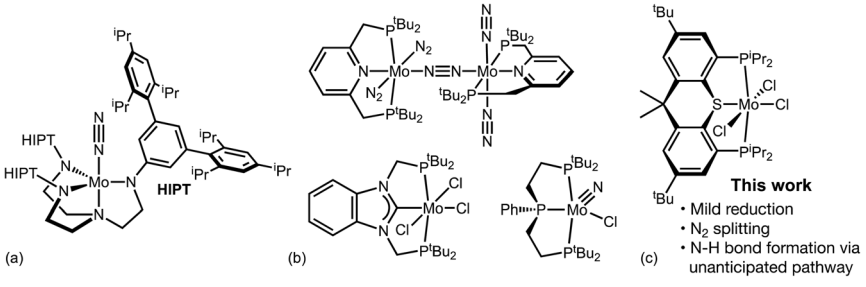


Fig. 1 (a) Schrock's (triamidoamine)Mo catalyst.[19,104] (b) (PYP)Mo catalysts or catalyst precursors reported by Nishibayashi.[20–37] (c) (PSP)Mo complex reported in this work.

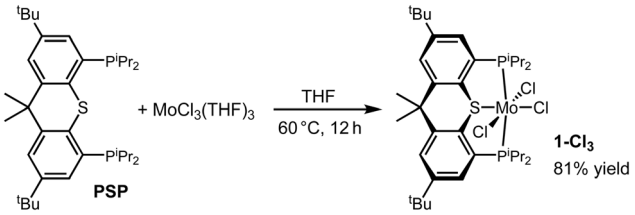


Scheme 1 Synthesis of (PSP)$MoCl_3$ (**1-$Cl_3$**).

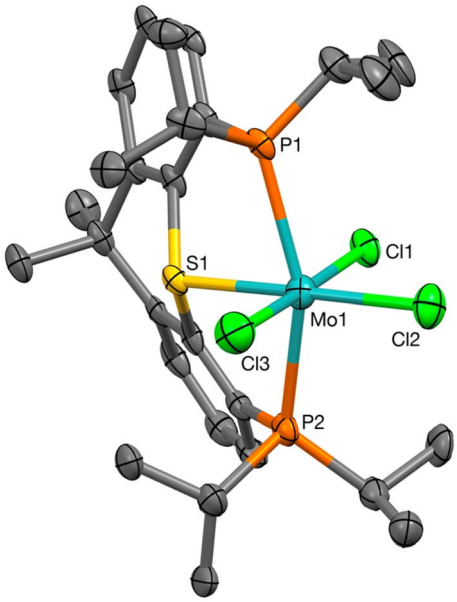


Fig. 2 ORTEP representation (50% probability ellipsoids) of the structure of **1-$Cl_3$** determined by X-ray diffraction; hydrogen atoms and PSP *t*-butyl groups omitted for clarity. Selected bond lengths (Å) and angles (°): Mo1–S1, 2.473; Mo1–P1, 2.563; Mo1–Cl1, 2.435; Mo1–Cl2, 2.394; Mo1–Cl3, 2.358; S1–Mo1–P1, 76.99; S1–Mo1–P2, 76.04; P1–Mo1–P2, 152.81; S1–Mo1–Cl1, 84.18; Cl1–Mo1–Cl2, 90.64; Cl2–Mo1–Cl3, 91.04; Cl3–Mo1–S1, 94.18.

The coordination sphere of Mo in **1-$Cl_3$** is approximately octahedral, with the $SMoCl_3$ unit being almost perfectly planar, although, as is typical with PXP-type pincer ligands, the X–M–P (S–Mo–P) angles are significantly less than 90°, at 76.5 ± 0.5°.

### Reduction of 1-$Cl_3$ and binding of $N_2$

Cyclic voltammetry of **1-$Cl_3$** in THF revealed a reversible reduction with a half-wave potential, $E_{1/2} = -1.56$ V *vs.* $Fc^{+/0}$. This reduction is *ca.* 400 mV less negative than that of (PNP)$MoCl_3$ ($E_{1/2} = -1.94$ V *vs.* $Fc^{+/0}$),[55] confirming our hypothesis that the PSP ligand would support milder reductions. Although no diamagnetic impurities or additional paramagnetic species were apparent by $^1$H NMR spectroscopy, an additional feature in the CV indicated a possible impurity at 10% or less. The major reduction peak was fully reversible at all scan rates studied, suggesting that chloride dissociation occurs relatively slowly. Chemical reductions were then attempted with sodium metal, which can assist in chloride abstraction *via* precipitation of NaCl.

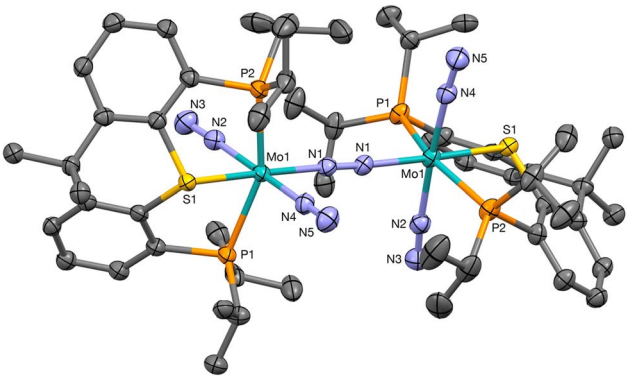


Fig. 3 ORTEP representations (50% probability ellipsoids) of the structure of **2** determined by X-ray diffraction; hydrogen atoms and PSP *t*-butyl groups omitted for clarity. Selected bond lengths (Å) and angles (°): N1–N1, 1.114; Mo1–N1, 2.067; Mo1–N2, 2.044; Mo1–N4, 2.023; N2–N3, 1.109; N4–N5, 1.113; Mo1–P1, 2.447; Mo1–P2, 2.436; P1–Mo1–S1, 79.0; P2–Mo1–S1, 79.5; P1–Mo1–P2, 156.7.

A THF solution of **1-$Cl_3$** was stirred over Na/Hg amalgam (0.5% w/w Na; 3 equiv. Na) under $N_2$ atmosphere. The predominant product exhibited broad signals in the $^{31}P\{^1H\}$ NMR spectrum; upon cooling, these resolved into an AB pattern of doublets at $\delta$ 80.8 and $\delta$ 79.1, $^2J_{PP} = 122.3$ Hz (Fig. S1†). Crystals were obtained and scXRD revealed a dimolybdenum product analogous to Nishibayashi's $Mo^0$ dimer [(PNP)$Mo(N_2)_2]_2(\mu\text{-}N_2)$,[23,32,33] *i.e.* [(PSP)$Mo(N_2)_2]_2(\mu\text{-}N_2)$ (**2**) (Fig. 3 and Scheme 2). Note that the bowl shape of the PSP ligand, in contrast with the planar PNP ligand, combined with the orthogonal relationship of the two PSP planes, results in the loss of mirror symmetry, rendering the P atoms of each PSP ligand inequivalent in accord with the predominant species observed in the $^{31}$P NMR spectrum.

In addition to the AB doublets, a sharp singlet at $\delta$ 78.2 (Fig. S1†) is seen in the $^{31}P\{^1H\}$ NMR spectrum of the solution under $N_2$ atmosphere. We attribute this to an equilibrium between **2** and mononuclear product (PSP)$Mo(N_2)_3$ (**3**; Scheme 2); such an equilibrium is expected from complex **2** as its $Mo(\mu\text{-}N_2)Mo$ core is a 12-π-electron system.[63] Accordingly, increased $N_2$ pressure led to an increased ratio of [**3**]:[**2**] which was reversed upon decreasing $N_2$ pressure. (The reaction kinetics were not measured, but it took approximately one week to reach apparent equilibrium, even with periodic rotation of the NMR tube to ensure gas-solution equilibration of $N_2$.) At $N_2$ pressures of 1.0 and 7.12 atm, $K_{eq}$ for the interconversion of **2** and **3**, as shown in Scheme 2, was determined by $^{31}P\{^1H\}$ NMR spectroscopy to be $3.4(1) \times 10^{-3}$ M $atm^{-1}$ (see ESI†).

The $^{31}P\{^1H\}$ NMR spectrum of the reaction solution additionally showed unidentified signals at *ca.* $\delta$ 77. Redissolving the crystals obtained as noted above affords a $^{31}P\{^1H\}$ NMR spectrum similar to that obtained before recrystallization. This leads us to speculate that the unidentified signals may be assigned to one or more isomers of **2** present in equilibrium in solution, *e.g.* isomers in which the bridging $N_2$ is positioned cis to S in one or both of the (PSP)Mo units.[22,64–66]

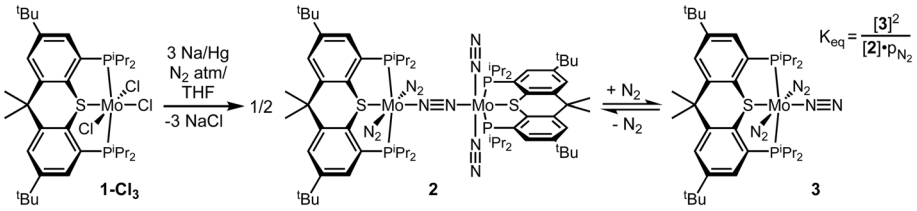


Scheme 2 Reaction of **1-Cl$_3$** with Na (3 equiv.) under $N_2$ atmosphere.

Admitting a CO atmosphere to the solution of **2** and **3** resulted in a $^{31}$P NMR spectrum indicating formation of two species, one manifesting a very broad AB doublet ($\delta$ 88.8 and $\delta$ 88.0), and the other a sharp singlet at $\delta$ 91.0. Two products were crystallized from this mixture and both were characterized by scXRD (see ESI†). One was found to be (PSP)Mo(CO)$_3$. The other was the $N_2$-bridging dimer [(PSP)Mo(CO)$_2$]$_2$($\mu$-$N_2$) (see ESI†), which is the analog of the product of the reaction of [(PNP)Mo($N_2$)$_2$]$_2$($\mu$-$N_2$)[20,23,32,33] with CO.[20]

## Reduction of 1-Cl$_3$ with cleavage of $N_2$

The Mo$^0$ dinitrogen complex **2** described above is stable with respect to the dissociative cleavage reaction to form metal nitrides, as expected based on the number of electrons in $\pi$-symmetry orbitals.[67] A $N_2$-bridged complex with one less e$^-$ per Mo would have the appropriate electronic structure for splitting, and iodide additives have previously been found to promote nitride formation in pincer Mo complexes.[32,38,40,43,44,64] Accordingly, **1-Cl$_3$** was treated with two reducing equivalents per Mo, rather than three as in the above examples, in the presence of added iodide. Under $N_2$ atmosphere, Na/Hg amalgam (0.5% w/w Na; 2 equiv. Na) was added to a THF solution of **1-Cl$_3$** and NaI (2 equiv.). The $^{31}$P{$^1$H} NMR spectrum of the resulting solution showed a single resonance, at $\delta$ 79.8, and the $^1$H NMR spectrum was consistent with a single diamagnetic PSP-containing species with $C_s$ symmetry.[68] When the reaction was conducted under $^{15}N_2$ atmosphere the resulting $^{15}$N NMR spectrum showed a single resonance at $\delta$ 446 (*cf.* $\delta$ 460 for (PNP)Mo(N)I[28]). These spectroscopic data are consistent with assignment as the product of $N_2$-cleavage, (PSP)Mo(N)I (**1-(N)I**, Scheme 3). Crystals were grown from benzene/pentane, and scXRD afforded the structure shown in Fig. 4. The complex **1-(N)I** has a coordination geometry that may be viewed as pseudo-square-pyramidal[38] with nitride in the apical position and an N–Mo–L angle of *ca.* 100° with each of the four other Mo-coordinating atoms. This structural motif is well precedented among pincer-Mo[38,69,70] and related nitride complexes.[71,72]

Based on the modest reduction potential of **1-Cl$_3$** ($E_{1/2}$ = −1.56 V *vs.* Fc$^{+/0}$), milder reductants should also be viable. Accordingly, under otherwise identical conditions, similar results were obtained with the use of 2 equiv. decamethylcobaltocene (Cp*$_2$Co), which has an oxidation potential of −1.94 V *vs.* Fc$^{+/0}$, as reductant in place of Na/Hg amalgam. However, no reaction was obtained with Cp$_2$Co (−1.33 V *vs.* Fc$^{+/0}$).

Thus, cleavage of $N_2$ occurs upon reaction of two equivalents of reductant with **1-Cl$_3$** while the addition of more than two equivalents leads to a stable bridging-$N_2$ dimolybdenum(0) complex. This is consistent with the well-established principle that bimetallic cleavage of $N_2$ to give nitrides is generally limited to bridging-$N_2$ complexes with 10 electrons in the M($\mu$-$N_2$)M $\pi$-system[12,41,66,67,73–76] (Scheme 4).

## Protonation of the nitride ligand of 1-(N)I

Having observed cleavage of the $N_2$ bond to give nitride complex **1-(N)I**, we considered likely subsequent steps in a potential

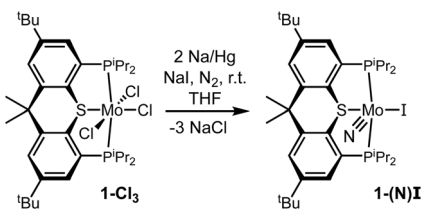


Scheme 3 Reduction of **1-Cl$_3$** by 2e$^-$ under $N_2$ atmosphere leading to cleavage of $N_2$.

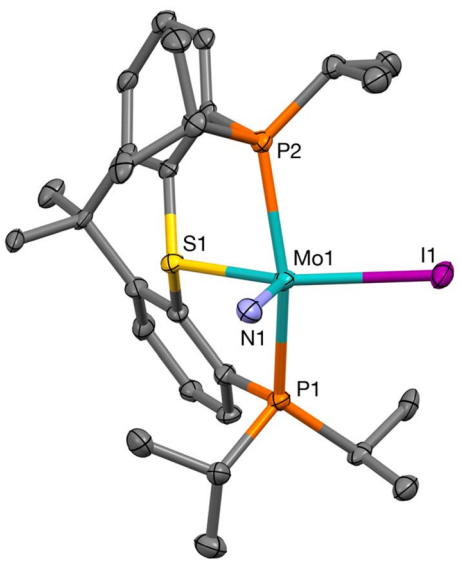


Fig. 4 ORTEP representations (50% probability ellipsoids) of the structure of **1-(N)I** determined by X-ray diffraction; hydrogen atoms and PSP *t*-butyl groups omitted for clarity. Selected bond lengths and angles: Mo1–N1, 1.648; Mo1–S1, 2.353; Mo1–I1, 2.815; Mo1–P1, 2.517; N1–Mo1–S1, 101.12; N1–Mo–I1, 107.26; N1–Mo1–P1, 99.73; N1–Mo1–P2, 99.34; P1–Mo1–P2, 152.55; S1–Mo–I1, 151.62.

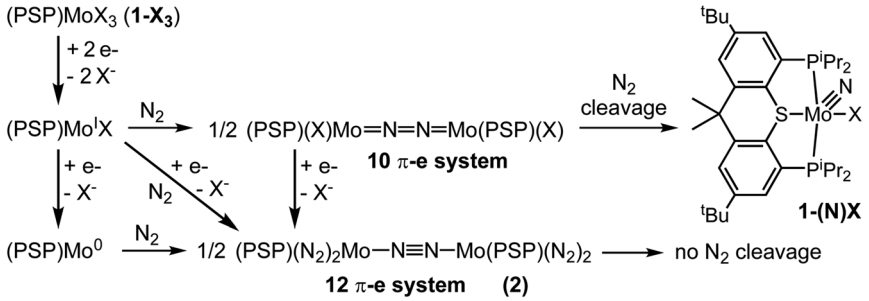


Scheme 4 Reduction of **1-X$_3$** by 2e$^-$ or 3e$^-$ under $N_2$ atmosphere. Hypothetical pathways to **1-(N)X** and **2**.

catalytic cycle for ammonia synthesis. As will be discussed in depth in following sections, formation of the initial N–H bond is indicated by DFT calculations to be the thermodynamically most challenging step in the conversion of the nitride to ammonia. Accordingly, **1-(N)I** did not react with the H-atom donor TEMPO-H (up to 5 equiv.) even after 2 days at room temperature. Likewise it did not react with H-atom donors $CpCr(CO)_3H$ (Cr–H BDFE = 54.9 kcal mol$^{-1}$ in MeCN[77]) or 1,4-cyclohexadiene (C–H BDFEs for benzene formation = 67.8 and 13.8 kcal mol$^{-1}$ in gas phase[77]). Moreover, **1-(N)I** did not undergo reaction with one-electron reductants $Cp_2Co$ or $Cp^*_2Co$ (1 equiv.) in the absence of a proton source such as [LutH]Cl, and cyclic voltammetry revealed a significantly negative reduction potential ($E_{pc} < -2.7$ V *vs.* $Fc^{+/0}$; Fig. S36†). We therefore undertook investigation of protonation as the initial N–H bond formation step.

The reaction of **1-(N)I** with Brookhart's acid[78] $[H(Et_2O)_2][BAr^F_4]$ ($Ar^F$ = 3,5-bis(trimethyl)phenyl) in THF appears to result in complete protonation (eqn (1)). The $^{31}P\{^1H\}$ NMR spectrum shows a single broad signal upon addition of 1.0 equiv. $[H(Et_2O)_2][BAr^F_4]$ at $\delta$ 67.3. Addition of two more equiv. of the acid has no discernible effect on the chemical shift although the signal is then sharp. Reaction of $[H(Et_2O)_2][BAr^F_4]$ with $^{15}N$-labeled **1-($^{15}$N)I** leads to a doublet ($\delta$ 51.0, $^1J_{HN}$ = 73 Hz) in the $^{15}N$ NMR spectrum, which is well precedented in work by Schrock as a protonated nitride.[79] The $^{31}P\{^1H\}$ NMR spectrum of **1-($^{15}$N)I** shows a doublet with a small $^{31}P$–$^{15}N$ coupling, $^2J_{PN}$ = 5.8 Hz.

$$\text{(PSP)Mo(I)N} + [H(Et_2O)_2][BAr^F_4] \rightarrow [\text{(PSP)Mo(I)NH}]^+[BAr^F_4]^- + 2Et_2O \quad (1)$$

Upon addition of one equiv. of a weaker acid, [LutH][OTf] (the most commonly used proton source in the context of this chemistry[32,33]), the characteristic peak of **1-(N)I** in the $^{31}P\{^1H\}$ NMR spectrum at $\delta$ 79.78 was broadened but only slightly shifted, to $\delta$ 79.2. An extremely broad peak appeared in the $^1H$ NMR spectrum at *ca.* $\delta$ 14.9. Addition of two more equiv. [LutH][OTf] resulted in a shift of the $^{31}P$ NMR signal to $\delta$ 77.8, while the downfield $^1H$ NMR peak shifted to $\delta$ 14.8 and became more intense and sharper. With a total of 12 equiv. [LutH][OTf] added, the $^{31}P$ NMR signal appeared at *ca.* $\delta$ 75.1 (see Fig. S2 and S3†) while the downfield $^1H$ NMR signal, clearly exchanging with free [LutH][OTf], was at $\delta$ 14.04. These results are consistent with protonation of **1-(N)I**, presumably at the nitride ligand, in a rapid equilibrium lying toward the left, either with the triflate anion coordinated to Mo (eqn (2a)) or ion-paired to the resulting cation (eqn (2b)). They are also consistent with an equilibrium in which the lutidinium cation is engaged in hydrogen bonding, again presumably with the nitride ligand (eqn (2c)).

$$\textbf{1-(N)I} + [LutH]^+[OTf]^- \rightleftharpoons \text{(PSP)Mo(I)(NH)(OTf)} + Lut \quad (2a)$$

$$\textbf{1-(N)I} + [LutH]^+[OTf]^- \rightleftharpoons [\text{(PSP)Mo(I)(NH)(Lut)}]^+[OTf]^- \quad (2b)$$

$$\textbf{1-(N)I} + [LutH]^+[OTf]^- \rightleftharpoons [\text{(PSP)Mo(I)N}\cdots\text{HLut}]^+[OTf]^- \quad (2c)$$

The addition of 4 equiv. lutidine to the solution with 12 equiv. [LutH][OTf] (with a $^{31}P$ NMR signal at *ca.* $\delta$ 75.1) yielded a signal at $\delta$ 79.1, essentially the chemical shift of the solution with 1 equiv. [LutH][OTf] ($\delta$ 79.2, close to that of free **1-(N)I**, $\delta$ 79.8). Since free lutidine participates only in the equilibrium of eqn (2a) this strongly supports eqn (2a), over eqn (2b) or (2c), as a description of the reaction of **1-(N)I** with [LutH][OTf]. Note however that this does not offer insight into the configuration of (PSP)Mo(I)(NH)(OTf), and in particular does not distinguish between a complex with $OTf^-$ coordinated to Mo *versus* an ion pair (likely with $OTf^-$ hydrogen-bonding to the N-bound proton).

The above results indicate that a very strong acid, such as $[H(Et_2O)_2][BAr^F_4]$, is required to fully protonate **1-(N)I** (to give **1-(NH)I$^+$**) while a moderately strong acid, [LutH][OTf], results in an equilibrium (likely with **1-(NH)I(OTf)**) that lies toward the unprotonated form. Remarkably, however, in contrast with the reaction with [LutH][OTf], addition of the chloride salt of the same acid, [LutH]Cl (3 equiv.), resulted in complete protonation with no observable equilibrium. The $^{31}P\{^1H\}$ NMR spectrum indicates the presence of two species in a *ca.* 4 : 1 ratio with chemical shifts of $\delta$ 63.9 and $\delta$ 64.9 respectively. The $^1H$ NMR spectrum contained signals at $\delta$ 6.40 and $\delta$ 6.49, also in a *ca.* 4 : 1 ratio, attributable to the protonated nitride ligand.

XRD of crystals grown by diffusion of pentane into a benzene solution yielded the molecular structure of ***trans*-1-(NH)(Cl)(I)** (Fig. 5). Apparently, by comparison with lutidinium triflate, in the case of lutidinium chloride coordination of the anion to molybdenum drives protonation of the nitride ligand fully to the protonated form (Scheme 5).

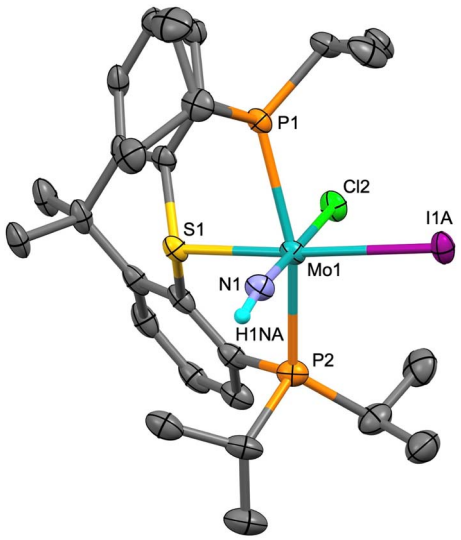


Fig. 5 ORTEP representations (50% probability ellipsoids) of the structure of *trans*-**1-(NH)(Cl)(I)** determined by X-ray diffraction; hydrogen atoms (other than the imido H), PSP *t*-butyl groups, and minor components of iodide site omitted for clarity. Fixed position of the imido proton determined from electron density map. Selected bond lengths (Å) and angles (°): Mo1–N1, 1.731; Mo1–S1, 2.372; Mo1–I1A, 2.837; Mo1–Cl2, 2.506; Mo1–P1, 2.503; Mo1–P2, 2.496; S1–Mo1–N1, 94.24; N1–Mo–I1A, 96.76; I1A–Mo1–Cl2, 86.44; P1–Mo–S1, 79.41.

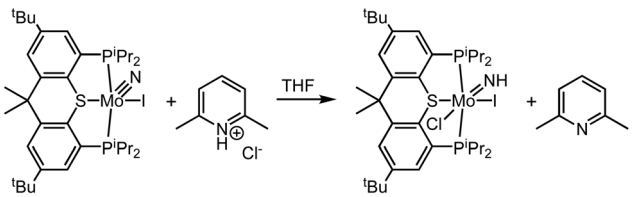


Scheme 5 Protonation of nitride ligand of **1-(N)I** *via* reaction with [LutH]Cl.

We propose that the minor species (with the $^{31}$P NMR chemical shift of $\delta$ 64.9 and $^{1}$H NMR shift of $\delta$ 6.49) is the corresponding dichloride complex, (PSP)MoCl$_2$(NH). In accord with this proposal, the crystal was disordered and the structure was solved as 18% (PSP)MoCl$_2$(NH).

[LutH]Cl (1.2 equiv.) was added to a THF-d$_8$ solution **1-($^{15}$N)I** to yield **1-($^{15}$NH)ICl**, which gave a $^{31}$P{$^{1}$H} NMR spectrum with signals, in a 4 : 1 ratio, at $\delta$ 63.5 and $\delta$ 64.4, both doublets with $^{2}J_{PN}$ = 6.1 Hz. The $^{1}$H NMR spectrum revealed a very sharp doublet of triplets at $\delta$ 6.31 with $^{1}J_{NH}$ = 73 Hz and $^{3}J_{PH}$ = 3.6 Hz attributable to the major species. In the $^{15}$N NMR spectrum a doublet appears at $\delta$ −2.5 ($^{1}J_{NH}$ = 73 Hz) (the signals were too broad to observe P–N coupling). The HSQC spectrum showed strong correlation of this $^{15}$N NMR signal with the $^{1}$H NMR signal at $\delta$ 6.31.

### Reaction of 1-(NH)ICl to yield ammonia, and the reverse reaction

In contrast with nitride **1-(N)I**, imide **1-(NH)ICl** was found to react with the H-atom donor TEMPO-H to give ammonia (Scheme 6). **1-(NH)ICl** was generated *in situ* by addition of 5 equiv. [LutH]Cl to a THF solution (2 mL) of **1-(N)I**; TEMPO-H (8 equiv.) was then added and after 24 h the volatiles were removed *in vacuo*. The residue was dissolved in DMSO-d$_6$ and $^{1}$H NMR spectroscopy revealed formation of ammonia (free and/or bound) that was detected as $NH_4^+$ in 88% yield. While this reaction does not afford definitive information about the thermodynamics of H$^\bullet$ transfer from TEMPO-H to **1-(NH)ICl** (in part because the nature of the Mo product was not determined), it appears that transfer of H$^\bullet$ from TEMPO-H to N does occur. Thus, although such H$^\bullet$ transfer is likely endergonic, it is not so uphill as to preclude the reaction from occurring (slowly) at room temperature, despite the relatively high O–H BDFE of TEMPO-H (65.5 kcal mol$^{-1}$ in THF[77]), and, importantly, in contrast with the lack of any reaction with nitride **1-(N)I**.[80]

Similarly, **1-(NH)ICl**, generated as described above, reacted with H-atom donors CpCr(CO)$_3$H (Cr–H BDFE = 54.9 kcal mol$^{-1}$ in MeCN[77]) and 1,4-cyclohexadiene (C–H BDFEs for benzene formation = 67.8 and 13.8 kcal mol$^{-1}$ in gas phase[77]); $NH_4^+$ was recovered in yields of 70% and 41% respectively (Scheme 6). As with TEMPO-H, **1-(N)I** showed no reactivity toward these species.

To further investigate the apparent tendency of **1-(NH)ICl** to react with H-atom donors, **1-(NH)ICl** was generated by the addition of [LutH]Cl (3 equiv.) to a THF-d$_8$ solution of **1-(N)I**. Cp$_2$Co (5 equiv.) was then added, over the course of 12 h. $^{1}$H NMR spectroscopy revealed appearance of the spectrum characteristic of paramagnetic **1-Cl$_3$** (which would likely overlap with a mixed halide complex, **1-Cl$_2$I**) and a signal at $\delta$ −0.02 attributable to $NH_3$ (Scheme 7). In a separate experiment (described in detail, S2.9.2†), volatiles from the resulting mixture were

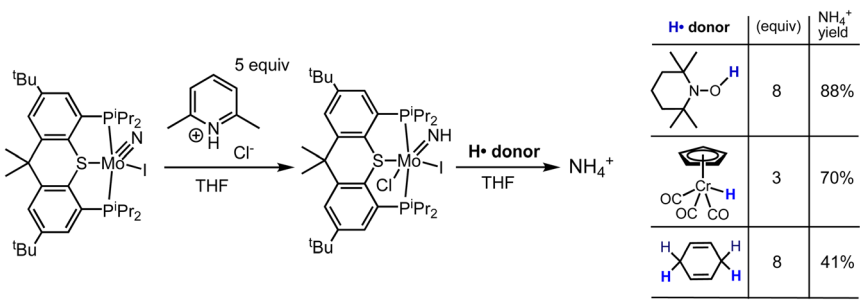


Scheme 6 Reaction of **1-(NH)ICl** with H-atom donors to yield ammonia.

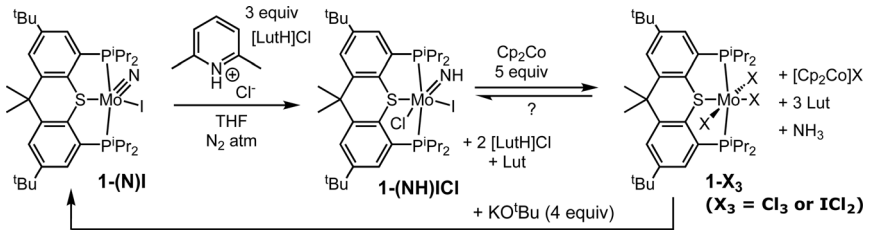


Scheme 7 Reaction of **1-(NH)ICl** with [LutH]Cl and $Cp_2Co$ to yield **1-Cl$_3$** and $NH_3$, followed by addition of KO$^t$Bu.

vacuum-transferred to a flask with HCl in diethyl ether; $^1$H NMR (DMSO-$d_6$) revealed a 30% yield of ammonia (as $NH_4^+$). Thus, while **1-(NH)ICl** undergoes no reaction with $Cp_2Co$ alone, it reacts with the PCET pair $Cp_2Co$/[LutH]Cl as shown in Scheme 7.

Although the stoichiometry of the reaction of Scheme 7 would only require a single equivalent of $Cp_2Co$, the reaction proceeded rapidly, but not to completion, even upon addition of excess (up to 5 equiv.) $Cp_2Co$. Considering the possibility that an equilibrium had been reached, we investigated the possibility of driving the reaction in reverse. Consistent with our hypothesis, addition of base (KO$^t$Bu, 4 equiv.) to the mixture formed in this experiment resulted in the reappearance of some starting material **1-(N)I** (Scheme 7; 17% yield).

The above experiments suggest, rather surprisingly, that the reaction of Mo$^{IV}$ complex **1-(NH)ICl** with $Cp_2Co$/[LutH]Cl to give **1-MoCl$_3$**, $Cp_2Co^+$, and ammonia, is reversible (Scheme 7).[81] Indeed, when [$Cp_2Co^+$][$PF_6^-$] (3 equiv.), $NH_3$ (2 equiv.) and KO$^t$Bu (4 equiv.) were added to a fresh solution of **1-Cl$_3$** in THF-$d_8$, the formation of $Cp_2Co$ was clearly observed in the $^1$H NMR spectrum ($\delta$ −50.5) within 18 h (Scheme 8). A signal at $\delta$ 77.2 in the $^{31}$P NMR spectrum is attributed to **1-(N)Cl** (identified by independent synthesis; see S2.11†) (*ca.* 25% of phosphorus-containing products). The presumed balanced equation is shown in Scheme 8. The major phosphorus-containing product, however, was the free PSP ligand (*ca.* 50%).

Thus, individual steps of reduction, $N_2$ cleavage (Schemes 2–5), and PCET or HAT, to give ammonium are demonstrated above. We have, however, thus far been unable to achieve catalysis to a significant extent with the (PSP)Mo unit. With **1-(N)I** as a prospective catalyst or precursor, the use of various pyridinium hydrohalide derivatives with $Cp^*_2Co$ was investigated. Slow addition (over 2 h) of 36 equiv. $Cp^*_2Co$ to a solution of **1-(N)I** and collidinium triflate (55 eq.) under $N_2$ atmosphere gave 1.29 equiv. $NH_4^+$; other attempts generally gave significantly less than one equivalent $NH_4^+$. While this may be related to the apparent proclivity of the PSP ligand to dissociate, as illustrated above, efforts are ongoing to more fully characterize the decomposition pathway.

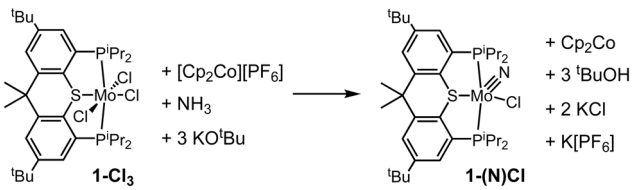


Scheme 8 Ideal balanced equation for reaction (oxidation) of **1-Cl$_3$** with $NH_3$, base, and $Cp_2Co^+$. (Actual reaction gives substantial decomposition/ligand-loss).

## Computational results and discussion of mechanism

The observations described above suggest potential intermediates and reaction steps of a catalytic pathway for the synthesis of ammonia from dinitrogen, proceeding *via* bimetallic dinitrogen cleavage and subsequent reaction of the resulting metal nitride (Scheme 9; Y = S). Our observations implicate a mechanism for conversion of nitride to ammonia that is fundamentally distinct from commonly proposed views. Herein we describe a computational study integrated with our experimental observations. To evaluate the generalities of our findings on (PSP)Mo, we expand the calculations to include comparisons with the archetypal (PNP)Mo-based system reported by Nishibayashi. The calculations were done using Gaussian 16.[82] The structures were optimized using the Minnesota-based hybrid metafunctional M06 [83] and Pople's split valence basis set 6-31G(d,p)[84,85] with the Stuttgart–Dresden effective core potential (SDD)[86] for heavy atoms (Mo, Co, Br, and I). Improved potential energies and bulk solvation effects were obtained from single-point calculations of the gas phase optimized geometries employing the M06 functional, the all-electron Karlsruhe basis set Def2-QZVP[86–90] for all atoms, and the SMD[91] dielectric continuum (with benzene as solvent model). The PSP ligand was modeled with an asymmetric derivative bearing *t*-butylmethylphosphino groups instead of bis(isopropyl)phosphino groups to avoid multiple conformational possibilities, while maintaining the same ligand steric profile.[92] Unless explicitly mentioned, this model has been used for all calculations pertinent to (PSP)Mo halide complexes. Bis(isopropyl)phosphino groups, however, were used for calculations involving the triflate anion to more precisely model the greater steric demands of the triflate ion and the absence of symmetry for triflate-coordinated and especially ion-paired triflate complexes. For the calculation of the inner-sphere reorganization energies associated with the

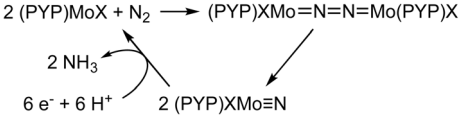


Scheme 9 Proposed pathway (highly simplified) for catalytic synthesis of $NH_3$ *via* bimetallic cleavage of $N_2$ and reduction/protonation.

calculation of kinetic barriers of electron transfer, the four-point method was used.[93] The computational methodologies are also discussed, in further detail, in the ESI.†

### Cleavage of $N_2$ by (PSP)Mo

Bimolecular cleavage of $N_2$ by (PSP)MoX to yield the corresponding nitride complex is central to the mechanism of catalysis implied in this work, in analogy to previous proposals for (PNP)Mo and other (pincer)Mo complexes.[12,17,32–36,52,66,94] In general, in the context of nitrogen fixation, cleavage of the strong $N_2$ bond is often presented as the origin of the great challenge to achieving conversion under mild conditions.[17,32,95–100] The barrier to bimolecular $N_2$ cleavage, however, is not necessarily particularly high nor rate-determining. For example, Yoshizawa and Nishibayashi have calculated that the free energy barrier ($\Delta G^{\ddagger}$) to $N_2$ cleavage by the bridged complex $[(PNP)MoI]_2(\mu\text{-}N_2)$ is only 21.8 kcal mol$^{-1}$, and that the reaction is exergonic by 27.6 kcal mol$^{-1}$.[28] Mézailles, Robert, and co-workers[52] have likewise calculated a barrier of 21.1 kcal mol$^{-1}$ for cleavage of $[(PPP)MoI]_2(\mu\text{-}N_2)$ (PPP = $\kappa^3$-PhP[$CH_2CH_2P(cy\text{-}C_6H_{11})_2$]$_2$); this reaction was calculated to be more exergonic (40.0 kcal mol$^{-1}$).

The activation free energy for $N_2$ cleavage by $[(PSP)MoI]_2(\mu\text{-}N_2)$ (Scheme 10; X = I), $\Delta G^{\ddagger}$ = 21.1 kcal mol$^{-1}$, is essentially equal to that of $[(PNP)MoI]_2(\mu\text{-}N_2)$ and $[(PPP)MoI]_2(\mu\text{-}N_2)$, while the reaction energy ($\Delta G^{\circ} = -33.7$ kcal mol$^{-1}$) is calculated to be intermediate between these two examples. The low calculated activation barrier is consistent with the rapid formation of **1-(N)I** observed upon the addition of 2.0 equivalents Na/Hg to **1-Cl$_3$** under $N_2$ atmosphere in the presence of NaI (Scheme 3). Slightly greater barriers are calculated for X = Br and Cl (Scheme 10). The origin of this effect of varying the halide ligand is not obvious,[101] and efforts are currently underway to elucidate it. In all cases the reaction is very exergonic.

### (PSP)MoN–H bond formation

It is typically presumed that the conversion of a nitride ligand to ammonia proceeds sequentially *via* H atom transfer (HAT) or PCET steps to yield the corresponding imide, amide, and ammonia complex (eqn (3)).[35–37,57,58]

As discussed above, within the class of complexes considered herein, the barriers to $N_2$ cleavage to form nitride are low, and the reaction is very exergonic (*i.e.* the nitride products are "low-energy" species). Therefore it would not be unexpected that conversion of nitride to ammonia would comprise the rate-determining segment of a catalytic cycle. Thus, for example, Nishibayashi has proposed that N–H bond formation can be rate-determining in the (PNP)Mo-catalyzed reduction of $N_2$ to $NH_3$.[35–37,57] More generally, insight into the reaction of nitride products to yield $NH_3$ is critical to the rational design of energy-efficient catalysts based on bimetallic $N_2$ splitting.[17,25,29,59,60]

Conversion of the nitride ligand to ammonia is also a key segment of catalytic pathways that are based on the so-called distal mechanism for $N_2$ reduction, first envisioned by Chatt[102,103] almost 50 years ago and many years later realized in practice by Yandulov and Schrock.[19,104–106] Indeed, it appears that most molecular catalysts for $N_2$ reduction based on molybdenum[20–28,30–33,38,107,108] (and very possibly many or most other metals[109,110]) operate *via* either bimolecular $N_2$-splitting or distal mechanisms; both classes require the conversion of a nitride ligand to ammonia.

**Formation of the "first" N–H bond ((PSP)MoN–H).** For the conversion of the nitride ligand of (PNP)Mo(N)(I) to coordinated ammonia, it has been shown that formation of the "first" NH bond is by far the thermodynamically least favorable of the three sequential bond formation steps indicated in eqn (3).[35–37,57,61] In other words, of the imide, amide, and ammonia complex in eqn (3), the imide has by far the lowest N–H BDFE. Our calculations of sequential H-atom addition to (PSP)Mo(N)(X) (Table 1) reveal the same trend as found for (PNP)Mo and other systems.[35–37,57,61] The first HAT is computed to afford a very weak N–H bond (BDFE = 31.6 kcal mol$^{-1}$, X = I; Table 1), while the BDFE of the N–H bonds resulting from the second and third H-atom addition are 58.2 and 49.3 kcal mol$^{-1}$, respectively. These N–H BDFEs are comparable to those calculated for the (PNP)Mo analogs (Table 1). In particular, the BDFEs of the first N–H bonds formed, *i.e.* those of complexes (PYP)Mo(I)(N–H), are essentially identical for Y = S or N, and in both cases these are the least thermodynamically favorable of the three N–H bonds, by a very significant margin (Table 1; BDFEs of (PYP)MoX[$NH_{(1-3)}$], Y = S, N). The very low calculated N–H BDFE

$$L_nM{\equiv}N \xrightarrow{H^+/e^-\ \text{or}\ H^{\cdot}} L_nM{=}NH \xrightarrow{H^+/e^-\ \text{or}\ H^{\cdot}} L_nM{-}NH_2 \xrightarrow{H^+/e^-\ \text{or}\ H^{\cdot}} L_nM{-}NH_3 \qquad (3)$$

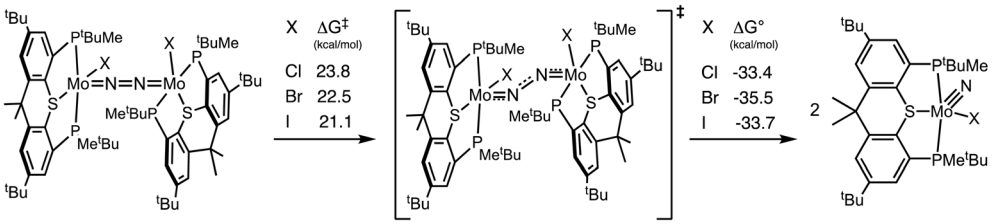


Scheme 10 Calculated activation barriers and reaction energies of cleavage of the $N_2$ bridge of $[(PSP)MoX]_2(\mu\text{-}N_2)$; X = Cl, Br, I.

Table 1 Calculated N–H BDFEs corresponding to sequential additions of H$^{\bullet}$ to (PYP)Mo$^{IV}$X(N); to (PYP)Mo$^{IV}$X$_2$(NH); and to [(PYP)Mo$^{IV}$X$_2$(NH)$^+$]; Y = S, N; X = Cl, I[a,b,c]

| Product | [Mo$^{III}$]X(N–H) | [Mo$^{II}$]X(NH–H) | [Mo$^{I}$]X(NH$_2$–H) | [Mo$^{III}$]X$_2$(NH–H) | [Mo$^{II}$]X$_2$(NH$_2$–H) | [Mo$^{III}$]X(NH–H)$^+$ | [Mo$^{II}$]X(NH$_2$–H)$^+$ |
|---|---|---|---|---|---|---|---|
| **[Mo] = (PSP)Mo** | **(PSP)MoX(NH$_n$) (*n* = 1, 2, 3)** | | | **(PSP)MoX$_2$(NH$_n$) (*n* = 2, 3)** | | **(PSP)MoX(NH$_n$)$^+$(*n* = 2, 3)** | |
| X = Cl | 33.0$^{d}$ | 56.3$^{t}$ | 51.2$^{d}$ | 50.0$^{q}$ | 55.9$^{t}$ | 47.0$^{q}$ | 60.7$^{t}$ |
| X = I | 31.6$^{d}$ | 58.2$^{t}$ | 49.3$^{d}$ | 49.1$^{q}$ | 58.3$^{t}$ | 45.7$^{q}$ | 47.7$^{t}$ |
| **[Mo] = (PNP)Mo** | **(PNP)MoX(NH$_n$) (*n* = 1, 2, 3)** | | | **(PNP)MoX$_2$(NH$_n$) (*n* = 2, 3)** | | **(PNP)MoX(NH$_n$)$^+$(*n* = 2, 3)** | |
| X = Cl | 31.2$^{d}$ | 45.0$^{s}$ | 52.9$^{d}$ | 50.7$^{q}$ | 50.7$^{t}$ | 47.8$^{q}$ | 54.0$^{t}$ |
| X = I | 31.9$^{d}$ | 45.8$^{s}$ | 51.3$^{d}$ | 50.6$^{q}$ | 51.5$^{t}$ | 47.8$^{q}$ | 52.7$^{t}$ |

[a] SMD$_{benzene}$/M06/Def2-QZVP//M06/SDD/6-31G(d,p). [b] Values in kcal mol$^{-1}$. [c] Mo(IV) species have singlet spin states. s = singlet, d = doublet, t = triplet, q = quartet spin states.

of (PSP)Mo(I)(N–H) is consistent with our experimental observation that H-donors such as TEMPO-H and CpCr(CO)$_3$H do not react with **1-(N)I**.

In the case of (PNP)Mo(N)X it has been suggested that formation of the first N–H bond may proceed *via* an initial one-electron reduction.[28] For **1-(N)X**, however, we calculate that transfer of an electron from the strong reducing agent Cp*$_2$Co, to give the ion-pair [Cp*$_2$Co][(PSP)Mo(N)X], is highly endergonic, ($\Delta G^\circ$ = 35.5, 36.7, and 35.5 kcal mol$^{-1}$ for X = Cl, Br, I respectively). (See Computational section for discussion of ion-pairing effects, without which the electron transfer would be even much more endergonic, calculated as 52.5, 52.8, and 52.2 kcal mol$^{-1}$ for X = Cl, Br, I respectively.) We also calculate that reduction of (PNP)Mo(N)X by Cp*$_2$Co is similarly unfavorable (Table S7.15†).

The calculated thermodynamic barrier for this one-electron reduction (*e.g.* $\Delta G^\circ$ = 35.5 kcal mol$^{-1}$ for X = I) is prohibitively high for a reaction to occur at ambient conditions, even before considering the kinetic barrier. Nevertheless, we wished to investigate the kinetic barrier, at least to the extent that computational methods would allow. The reorganization energies ($\lambda_0$) were calculated for Cp*$_2$Co/[Cp*$_2$Co$^+$] and for (PSP)Mo(N)X/[(PSP)Mo(N)X$^-$] and from these values the kinetic barriers to electron transfer could be calculated using the Marcus equation (eqn (4)).

$$\Delta G^{\ddagger} = \frac{(\lambda_0 + \Delta G^\circ)^2}{4\lambda_0} \quad (4)$$

The values of $\Delta G^{\ddagger}$ for reduction of **1-(N)X** by Cp*$_2$Co were determined, according to eqn (4), to be 53.3, 56.5, and 54.2 kcal mol$^{-1}$ (X = Cl, Br, I respectively). Clearly these represent a prohibitively high kinetic barrier but, again, even absent any barrier in addition to the calculated endergonicity (*e.g.* $\Delta G^\circ$ = 35.5 kcal mol$^{-1}$ for X = Cl, I), the rate at ambient temperature would be extremely slow: $6 \times 10^{-14}$ s$^{-1}$ at 25 °C.

In agreement with these conclusions, as noted above, **1-(N)I** underwent no reaction with Cp$_2$Co or even Cp*$_2$Co in the absence of a proton source such as [LutH]Cl, and cyclic voltammetry revealed a significantly negative reduction potential ($E_{pc} < -2.7$ V *vs.* Fc$^{+/0}$; S36†).

We therefore considered protonation, rather than reduction, following cleavage of $N_2$.[94] In the case of (PSP)Mo, as discussed above, experimentally we observed that the equilibrium for protonation of the $N_2$ cleavage product **1-(N)(I)** by [LutH][OTf] is slightly unfavorable, while [LutH]Cl readily reacted to afford an imide complex **1-(NH)(I)(Cl)** without any indication of an observable equilibrium. Our DFT calculations are quite consistent with these observations. The reaction of **1-(N)(I)** with [LutH]Cl to give *trans*-**1-(NH)(Cl)(I)** is calculated to be exergonic, $\Delta G^\circ$ = −11.8 kcal mol$^{-1}$ (eqn (5), X = Cl), whereas the analogous reaction with [LutH][OTf] is very slightly endergonic, $\Delta G^\circ$ = 0.2 kcal mol$^{-1}$.

$$(\mathrm{PSP})\mathrm{Mo(N)I} + [\mathrm{LutH}]\mathrm{X} \rightarrow (\mathrm{PSP})\mathrm{Mo(NH)(I)(X)} + \mathrm{Lut} \quad \begin{matrix} \mathrm{X = Cl:}\ \ \Delta G^\circ = -11.8\ \text{kcal mol}^{-1} \\ \mathrm{X = OTf:}\ \ \Delta G^\circ = 0.2\ \text{kcal mol}^{-1} \end{matrix} \quad (5)$$

Note that even the calculated endergonic reaction with [LutH][OTf] is promoted by coordination of the corresponding anion (OTf$^-$), although less so than is found for the more strongly coordinating chloride anion. The isomeric N-protonated species without Mo-coordinated triflate, but with triflate hydrogen-bonding to the NH ligand instead, was calculated to be higher in free energy, $\Delta G^\circ$ = 7.1 kcal mol$^{-1}$ (eqn (6)). **1-(N)(I)** that is unprotonated, but acting as a H-bonding acceptor with [LutH][OTf], was calculated to be slightly lower in free energy, $\Delta G^\circ$ = 5.1 kcal mol$^{-1}$ (eqn (7)), but still higher in energy than the triflate-coordinated product of eqn (5). These results convey the favorability of N-protonation combined with anion coordination and the greater magnitude of this effect ($\Delta\Delta G^\circ_{calc}$ = 12.0 kcal mol$^{-1}$) with chloride *versus* triflate anion (eqn (5)).

$$(PSP)Mo(N)I + [LutH^+][OTf^-] \rightarrow (PSP)Mo(I)(NH)^+\cdots OTf^- + Lut,\ \Delta G^\circ_{calc} = 7.1\ kcal\ mol^{-1} \quad (6)$$

$$(PSP)Mo(N)I + [LutH^+][OTf^-] \rightarrow [(PSP)Mo(I)(N)\cdots HLut][OTf],\ \Delta G^\circ_{calc} = 5.1\ kcal\ mol^{-1} \quad (7)$$

Thus, the calculated unfavorable thermodynamics of one-electron reduction of **1-(N)(I)** are experimentally manifest by the lack of reaction with the strong reductant $Cp^*_2Co$. Likewise, the very low calculated N–H BDFE of **1-(NH)(I)** is consistent with the failure of **1-(N)(I)** to react with H-atom donors, TEMPO-H (O–H BDFE = 65.5 kcal $mol^{-1}$ in THF[77]), 1,4-cyclohexadiene (C–H BDFEs = 67.8, gas phase[77]) or even $CpCr(CO)_3H$ (Cr–H BDFE = 54.9 kcal $mol^{-1}$, MeCN[77]). Protonation, however, is achievable and kinetically very facile, assisted by coordination of an anion. Importantly, while protonation of course constitutes the formation of an N–H bond, it is not the reverse of the homolytic N–H bond dissociation that is implied to be so challenging based on the low N–H BDFE of **1-(NH)(I)**. Protonation does not represent a "full formation of the first N–H bond" in the sense of HAT or PCET as indicated in eqn (3).

**Formation of the second N–H bond ((PSP)MoNH–H).** Our initial experimental observations of nitride protonation involved the reaction of the iodide complex **1-(N)(I)** with the lutidinium chloride salt. For the purpose of analyzing a multi-step pathway, however, mixing halides complicates an already complicated set of possibilities with multiple possible permutations including isomers and halide exchange products. In the following discussion of the full conversion of nitride to $NH_3$ we will therefore consider the reaction of (PSP)Mo(N)(Cl) with [LutH]Cl and $Cp^*_2Co$. The complete and fully analogous pathways have also been calculated for the reactions of (PSP)Mo(N)(X) with [LutH]X for X = Br and I, in both cases favoring the same pathway as obtained with X = Cl and yielding the same conclusions with no qualitative differences (ESI†). We have also calculated pathways for N–H bond formation by [LutH][OTf] and $Cp^*_2Co$, subsequent to the reaction of **1-(N)(I)** with [LutH][OTf] to yield **1-(NH)(I)(OTf)**, with the calculations again favoring the same pathways. (See ESI Scheme S7.14†).

In a conventional protonation/reduction framework, in order to preserve charge balance, protonation of the nitride ligand would expectedly be followed by one-electron reduction. However, in the case of protonation of **1-(N)X** this cannot be assumed, as charge balance is maintained by addition of a second halide. We therefore consider two pathways for the formation of the second N–H bond, following protonation: pathway A, beginning with reduction, and pathway B beginning with (a second) protonation. The energy profiles of the two pathways are illustrated in Fig. 6.

Following the net addition of HCl to **1-(N)Cl**, transfer of an electron from $Cp^*_2Co$ to **1-(NH)$Cl_2$**, to give the ion-pair $[Cp^*_2Co][(PSP)Mo(NH)Cl_2]$, is calculated to be highly unfavorable, $\Delta G^\circ$ = 28.7 kcal $mol^{-1}$ (eqn (8), and pathway A in Fig. 6). This is consistent with the failure of **1-(NH)ICl** to undergo reaction with $Cp^*_2Co$ in the absence of [LutH]Cl and cyclic voltammetry experiments on **1-(NH)ICl** showing irreversible reductions only at very negative potentials (Fig. S37†).

$$Cp^*_2Co + (PSP)Mo(NH)X_2 \rightarrow [Cp^*_2Co^+][(PSP)Mo(NH)X_2^-],\ X = Cl;\ \Delta G^\circ = 28.7\ kcal\ mol^{-1} \quad (8)$$

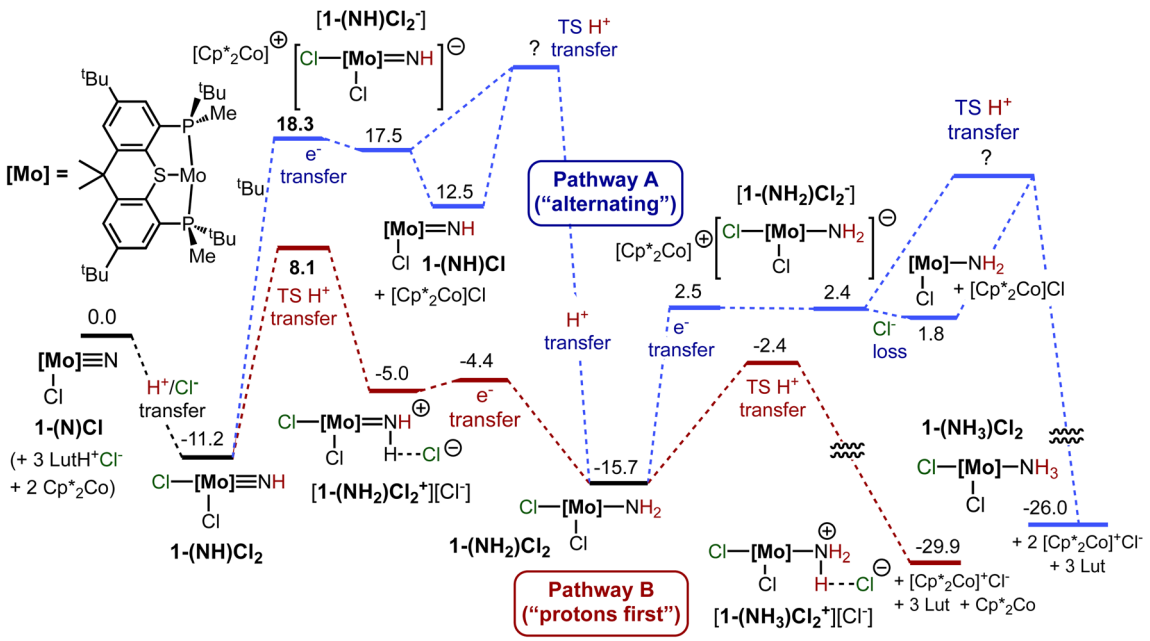


Fig. 6 Gibbs free energy profile (kcal $mol^{-1}$) for calculated pathways for the conversion of the nitride ligand of (PSP)Mo(N)Cl to ammonia (the formation of three N–H bonds). The "protons-first" pathway (red), comprising the addition of $Cl^-$, three $H^+$, and one $e^-$, $H^+(Cl^-)/H^+/e^-/H^+$ (*i.e.* PT–PT–ET–PT), has an overall barrier at least 10.2 kcal $mol^{-1}$ less than that of the "alternating" pathway (blue), addition of $H^+(Cl^-)/e^-/H^+/e^-/H^+$ (*i.e.* PT–ET–PT–ET–PT).

Using the same Marcus-theory based approach as described above to estimate the kinetics of one-electron reduction of **1-(N)X**, $\Delta G^{\ddagger}$ for reduction of **1-(NH)Cl$_2$** by Cp*$_2$Co was determined to be 29.5 kcal mol$^{-1}$ (Fig. 6, pathway A). Given the limitations of Marcus theory[111,112] and assuming that the thermodynamic value of $\Delta G^{\circ} = 28.7$ kcal mol$^{-1}$ must be viewed as a calculated lower limit, we suspect that the kinetics of the electron transfer step would be slower than are indicated by this calculated value of $\Delta G^{\ddagger}$. Nevertheless even the rate predicted assuming that $\Delta G^{\ddagger} = 29.5$ kcal mol$^{-1}$ would be prohibitively slow at ambient temperature ($1.5 \times 10^{-9}$ s$^{-1}$ at 25 °C).

Subsequent loss of chloride from the hypothetical ion-paired product of electron-transfer, [Cp*$_2$Co$^+$][(PSP)Mo$^{III}$(NH)Cl$_2^-$], is calculated to be exergonic by 5.0 kcal mol$^{-1}$ (Fig. 6, pathway A; eqn (9b)), leading to the formation of (PSP)Mo(NH)Cl and [Cp*$_2$Co]Cl. The resulting overall reduction of (PSP)Mo$^{IV}$(NH)Cl$_2$ by Cp*$_2$Co is shown in eqn (9c).

$$(PSP)Mo^{IV}(NH)Cl_2 + Cp^*_2Co \rightarrow [Cp^*_2Co^+][(PSP)Mo^{III}(NH)Cl_2^-],\ \Delta G^{\circ} = 28.7 \text{ kcal mol}^{-1} \quad (9a)$$

$$[Cp^*_2Co^+][(PSP)Mo^{III}(NH)Cl_2^-] \rightarrow (PSP)Mo^{III}(NH)Cl + [Cp^*_2Co^+]Cl^-,\ \Delta G^{\circ} = -5.0 \text{ kcal mol}^{-1} \quad (9b)$$

$$(PSP)Mo^{IV}(NH)Cl_2 + Cp^*_2Co \rightarrow (PSP)Mo^{III}(NH)Cl + [Cp^*_2Co^+]Cl^-,\ \Delta G^{\circ} = 23.7 \text{ kcal mol}^{-1} \quad (9c)$$

The product of eqn (9c), (PSP)Mo$^{III}$(NH)Cl (**1-(NH)Cl**), is the net product of HAT/PCET to the starting nitride, **1-(N)Cl**, formed *via* addition of H$^+$/Cl$^-$ followed by reduction and loss of Cl$^-$ (pathway A, Fig. 6). While the barrier may be prohibitive ($\Delta G^{\ddagger} = 29.5$ kcal mol$^{-1}$), we calculate that if **1-(NH)Cl** were formed it could then react with [LutH]Cl, very exergonically, to undergo addition of H$^+$Cl$^-$ across the Mo$^{III}$=NH bond leading to amido complex (PSP)Mo$^{III}$(NH$_2$)Cl$_2$ (eqn (10) and Fig. 6, pathway A). The TS for the proton transfer from lutidinium chloride could not be located but even assuming that there is a negligible enthalpic barrier, the entropic contribution of a bimolecular reaction is expected to be significant (and similar to the high barrier determined for the (PNP)Mo system which is discussed below). Thermodynamically, the reaction of **1-(NH)Cl** with [LutH]Cl (eqn (10)) is calculated to be quite exergonic ($\Delta G^{\circ} = -28.2$ kcal mol$^{-1}$; Fig. 6, pathway A). Combined with eqn (9c) ($\Delta G^{\circ} = 23.7$ kcal mol$^{-1}$) this describes a reduction-first pathway for the thermodynamically favorable net addition of H-atom to the imide nitrogen of **1-(NH)Cl$_2$** to give **1-(NH$_2$)Cl$_2$** (eqn (10), $\Delta G^{\circ} = -4.5$ kcal mol$^{-1}$).

$$(PSP)Mo^{IV}(NH)Cl_2 + Cp^*_2Co + [LutH]Cl \rightarrow (PSP)Mo^{III}(NH_2)Cl_2 + [Cp^*_2Co^+]Cl^- + Lut,\ \Delta G^{\circ} = -4.5 \text{ kcal mol}^{-1} \quad (10)$$

The reduction of **1-(NH)Cl$_2$** on pathway A would clearly encounter a prohibitive barrier. In contrast, proton transfer from [LutH]Cl to **1-(NH)Cl$_2$** on pathway B is calculated to be kinetically facile and only slightly endergonic (eqn (11)). The kinetic barrier for this second protonation is calculated be $\Delta G^{\ddagger} = 19.3$ kcal mol$^{-1}$ (mostly attributable to entropy; $\Delta E^{\ddagger}$ is only 7.3 kcal mol$^{-1}$), which would permit a rapid reaction at room temperature.

$$\textbf{1-(NH)Cl}_2 + [LutH^+]Cl^- \rightarrow [\textbf{1-(NH}_2\textbf{)Cl}_2^+]Cl^- + Lut,\ \Delta G^{\ddagger} = 19.3 \text{ kcal mol}^{-1};\ \Delta G^{\circ} = 6.2 \text{ kcal mol}^{-1} \quad (11)$$

Subsequent reduction of the protonated complex [**1-(NH$_2$)Cl$_2$**]$^+$Cl$^-$ is calculated to be exergonic ($\Delta G^{\circ} = -10.7$ kcal mol$^{-1}$, eqn (12); Fig. 6, pathway B). Employing Marcus theory as discussed above, the kinetic barrier to electron transfer following this protonation is determined to be very low, $\Delta G^{\ddagger} = 0.6$ kcal mol$^{-1}$.

$$[\textbf{1-(NH}_2\textbf{)Cl}_2^+]Cl^- + Cp^*_2Co \rightarrow [Cp^*_2Co^+]Cl^- + \textbf{1-(NH}_2\textbf{)Cl}_2,\ \Delta G^{\ddagger} = 0.6 \text{ kcal mol}^{-1};\ \Delta G^{\circ} = -10.7 \text{ kcal mol}^{-1} \quad (12)$$

Thus, our results strongly indicate that conversion of the $N_2$-cleavage product, **1-(N)Cl**, to **1-(NH$_2$)Cl$_2$**, proceeds initially *via* N-protonation combined with addition of halide to Mo, as a rapid exergonic reaction to yield **1-(NH)Cl$_2$**. **1-(NH)Cl$_2$** then undergoes a slightly endergonic protonation to give [**1-(NH$_2$)Cl$_2^+$**]Cl$^-$ (eqn (11)). Reduction of this protonated complex by Cp*$_2$Co is calculated to be exergonic with a very low kinetic barrier (eqn (12)). The net reaction, PCET to **1-(NH)Cl$_2$** (eqn (10)) is exergonic by 4.5 kcal mol$^{-1}$. Very similar results are obtained for the reactions of **1-(N)X** and [LutH]X for X = Br and I (see ESI†).

Experimentally, consistent with the prediction of a very facile (and not rate-limiting) reduction of [**1-(NH$_2$)Cl$_2^+$**]Cl$^-$ by Cp*$_2$Co, even with use of the much weaker reductant, Cp$_2$Co (Scheme 7), the formation of the second (as well as third) N–H bonds proceeds readily. By contrast, a hypothetical reduction of neutral **1-(NH)Cl$_2$** by Cp$_2$Co, prior to protonation, would be far more endergonic than with Cp*$_2$Co ($\Delta E^{\circ} = 0.78$ eV = 18.1 kcal mol$^{-1}$). The "protons-first" pathway (Fig. 6, pathway B) is thus strongly favored, by computation and experiment, for the formation of the first two N–H bonds on the path of the conversion of nitride ligand to ammonia.

Thus pathway B does not follow the paradigm of eqn (3), but instead circumvents the formation of a "first N–H bond" in the sense of HAT/PCET to **1-(N)Cl**. Formation of Mo$^{III}$ imide **1-(NH)Cl** or its Cl$^-$ adduct [**1-(NH)Cl$_2^-$**] are avoided. Instead, subsequent to the first protonation (and halide addition), a second protonation occurs, followed by a reduction. This comprises, overall, HAT/PCET to the Mo$^{IV}$ imide **1-(NH)Cl$_2$**, forming an N–H bond with a BDFE of 49.1 kcal mol$^{-1}$. This is much more favorable than HAT/PCET to the Mo$^{IV}$ nitride **1-(N)Cl** (corresponding to a BDFE of 31.6 kcal mol$^{-1}$).

The underlying explanation for the much greater driving force ($\Delta\Delta G^{\circ} = 17.5$ kcal mol$^{-1}$) for HAT/PCET to Mo$^{IV}$ imide **1-(NH)Cl$_2$**, *versus* HAT/PCET to Mo$^{IV}$ nitride **1-(N)Cl**, is not obvious. Apparently, however, it can be primarily attributed to the added proton, rather than the coordinated halide. Thus HAT/PCET to the protonated Mo$^{IV}$ nitride, *i.e.* the cationic imide **1-(NH)Cl$^+$**, has a driving force (45.7 kcal mol$^{-1}$) similar to that for HAT/PCET to neutral **1-(NH)Cl$_2$** (49.1 kcal mol$^{-1}$) (Table 1). The major effect of the anion appears to be to favor this initial protonation of the nitride. It appears that HAT/PCET to nitride

ligands may be inherently much less favorable than HAT/PCET to imides, independent of the oxidation state of the metal. It is perhaps notable, however, that coordination of the chloride anion even slightly favors (49.1 *vs.* 45.7 kcal mol$^{-1}$) HAT/PCET – as this is formally a reduction of the molybdenum center.

The preference for pathway B *versus* pathway A is expected to apply even more strongly with a reducing agent weaker than Cp*$_2$Co as the reduction step is not rate-determining. Importantly, this may be extrapolated to the case of an electrochemical system in which the cathodic overpotential is not very high, as would be required of a practical energy-efficient system.[11]

**Formation of the third N–H bond ((PSP)MoNH$_2$–H).** Following formation of amido complex **1-(NH$_2$)Cl$_2$**, the "alternating motif" of pathway A (Fig. 6) would involve one-electron reduction followed by a third protonation. Reduction of **1-(NH$_2$)Cl$_2$** by Cp*$_2$Co is calculated to be endergonic by 18.1 kcal mol$^{-1}$, with a kinetic barrier calculated (using Marcus theory) to be 18.2 kcal mol$^{-1}$ (Fig. 6). Again, we were unable to locate a transition state for protonation of the resulting anion to give **1-(NH$_3$)Cl$_2$** but again, the unfavorable entropy of a bimolecular reaction would result in a significant addition to the barrier. But even when compared with only the free energy of the electron transfer ($\Delta G^\circ$ = 18.1 kcal mol$^{-1}$), the calculated kinetic barrier to protonation of **1-(NH$_2$)Cl$_2$** is lower, $\Delta G^\ddagger$ = 13.3 kcal mol$^{-1}$ and such protonation is highly exergonic ($\Delta G^\circ$ = −14.2 kcal mol$^{-1}$; Fig. 6, pathway B). Protonation of **1-(NH$_2$)Cl$_2$** will therefore be rapid and irreversible, affording the cationic ammonia complex [**1-(NH$_3$)Cl$_2$**]$^+$Cl$^-$. The calculated reaction barriers and free energies are very similar for the reactions of **1-(NH$_2$)X$_2$** to give [**1-(NH$_3$)X$_2$**$^+$]X$^-$ for X = Br ($\Delta G^\circ$ = −15.9 kcal mol$^{-1}$) and X = I ($\Delta G^\circ$ = −16.7 kcal mol$^{-1}$) (see ESI†).

As discussed above in regard to formation of the second N–H bond, the experimental observation that formation of the third N–H bond proceeds readily even with the weak reducing agent Cp$_2$Co instead of Cp*$_2$Co, argues that a reduction step does not contribute to a rate-determining barrier. Again this is consistent with a "protons first" pathway (Fig. 6, pathway B). Beginning with (PSP)Mo(N)X (**1-(N)X**), the overall pathway to NH$_3$ formation may therefore be described as addition of H$^+$/X$^-$/H$^+$/e$^-$/H$^+$.

Subsequent to the very exergonic third protonation *via* pathway B, displacement of NH$_3$ by Cl$^-$ (Scheme 11) is calculated to be exergonic by 10.5 kcal mol$^{-1}$, giving **1-Cl$_3$**, the complex with which we began our study. In a catalytic cycle, if this displacement of ammonia by chloride occurs it would necessarily be followed by one-electron reduction and loss of a halide ion (Scheme 11) – the presumed initial step in the reactions of Schemes 2 and 3. An alternative to the replacement of NH$_3$ by chloride (and subsequent reduction), would be direct one-electron reduction of the cationic species [**1-(NH$_3$)Cl$_2$**]$^+$Cl$^-$ (Scheme 11). This step leads to the last species shown to be formed in pathway A in Fig. 6, *i.e.* the neutral Mo$^{II}$ complex **1-(NH$_3$)Cl$_2$**, but with an overall free energy of activation much lower than that of pathway A (which proceeds *via* one-electron reduction of neutral **1-(NH$_2$)Cl$_2$**). Although beyond the scope of this work, further investigations are underway to determine

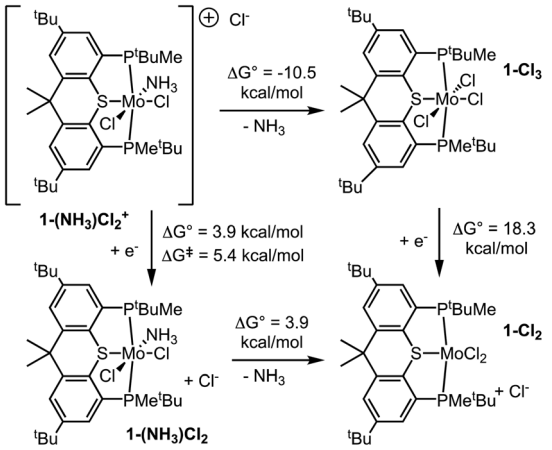


Scheme 11 Alternative pathways for loss of NH$_3$ and reduction by Cp*$_2$Co, subsequent to protonation of **1-(NH$_2$)Cl$_2$** by [LutH]Cl.

in detail the pathways for reduction, with chemical reductants and electrochemically, which ultimately lead from Mo$^{III}$ complexes [**1-(NH$_3$)X$_2$**$^+$] to the N$_2$-bridging dimolybdenum(I) complexes [(PSP)MoX](μ-N$_2$).

### Comparison with the (PNP)MoN system

Extending our computational approach to the iconic PNP system yields results that are very similar to those obtained for PSP. As in the case of the PSP system, the initial N–H bond formation, using [LutH]Cl as the source of H$^+$, is calculated to be exergonic (by 5.9 kcal mol$^{-1}$) when coupled with chloride coordination. This reaction appears to have no barrier on the electronic energy surface. A subsequent hypothetical one-electron reduction by Cp*$_2$Co is highly endergonic by 25.4 kcal mol$^{-1}$ (pathway A, Fig. 7). For protonation of the resulting anion, in contrast with the case of the PSP analog ([(PSP)Mo(NH)Cl$_2$]$^-$ anion), we successfully located a transition state; the free energy is 11.3 kcal mol$^{-1}$ above the ion pair (fully attributable to entropy). The overall barrier to e$^-$-transfer followed by protonation is therefore prohibitively high, 36.7 kcal mol$^{-1}$. In contrast, protonation of (PNP)Mo(NH)Cl$_2$ is slightly exergonic ($\Delta G^\circ$ = −2.0 kcal mol$^{-1}$) (pathway B, Fig. 7), with a relatively low barrier $\Delta G^\ddagger$ = 21.2 kcal mol$^{-1}$. One-electron reduction of the resulting [(PNP)Mo(NH$_2$)Cl$_2$$^+$]Cl$^-$ ion pair is also slightly exergonic, and with a very low calculated kinetic barrier of $\Delta G^\ddagger$ = 1.6 kcal mol$^{-1}$ as determined using Marcus theory (pathway B).

The "protons first" pathway B and the "alternating" pathway A reach the common intermediate (PNP)Mo(NH$_2$)Cl$_2$ analogously to the (PSP)Mo system. In the (PNP)Mo case our ability to locate a TS for the second protonation allows us to more quantitatively determine that the overall barrier for pathway A is significantly higher, by 15.5 kcal mol$^{-1}$ (30.8 kcal mol$^{-1}$ *versus* 15.3 kcal mol$^{-1}$), than that for pathway B (Fig. 7).

The intermediate common to both pathways A and B in Fig. 7, (PNP)Mo(NH$_2$)Cl$_2$, can undergo either protonation or reduction. As in the case of the (PSP)Mo system the barrier to reduction is not prohibitive, but protonation is much more

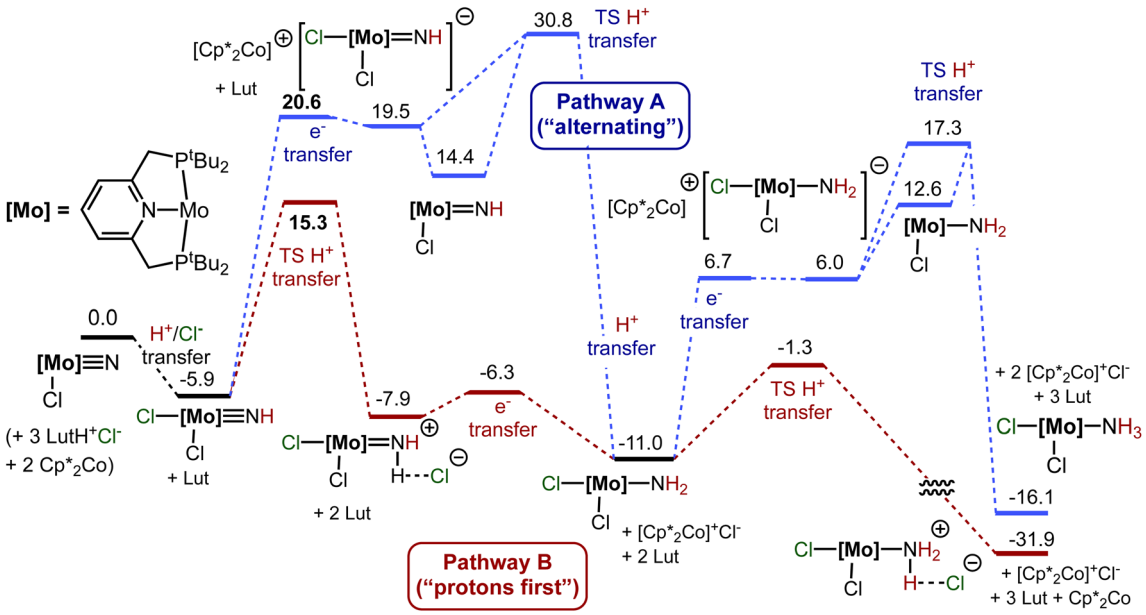


Fig. 7 Free energy profile (kcal mol$^{-1}$) for the two calculated pathways for the conversion of the nitride ligand of (PNP)Mo(N)Cl to ammonia (the formation of three N–H bonds). The "protons-first" pathway (red), comprising the addition of three $H^+$ and one $e^-$, $H^+(Cl^-)/H^+/e^-/H^+$, has an overall barrier that is 15.5 kcal mol$^{-1}$ less than that of the "alternating" pathway (blue), addition of $H^+/e^-/H^+/e^-/H^+$.

favorable than reduction, kinetically ($\Delta G^{\ddagger}$ = 9.7 kcal mol$^{-1}$ *vs.* 17.7 kcal mol$^{-1}$) and especially thermodynamically ($\Delta G°$ = −20.9 kcal mol$^{-1}$ *vs.* 17.0 kcal mol$^{-1}$). Moreover, as with formation of the second N–H bond, we have successfully located a TS for protonation subsequent to reduction (again, in contrast with the (PSP)Mo system) to form the third N–H bond. The overall barrier for the net addition of H-atom to (PNP)Mo(NH$_2$)Cl$_2$ *via* the reduction/protonation pathway is 28.3 kcal mol$^{-1}$ (pathway A). This compares with the much lower barrier of $\Delta G^{\ddagger}$ = 9.7 kcal mol$^{-1}$ for the very exergonic protonation yielding bound ammonia to afford the cationic complex [(PNP)Mo(NH$_3$)Cl$_2^+$] (pathway B).

Our calculations with the PNP ligand thus serve to (a) reinforce the conclusions obtained with (PSP)Mo, by enabling identification of the TSs for the 2nd and 3rd protonation in an otherwise quite similar pathway, and (b) to demonstrate the broader applicability of the findings obtained with PSP.

## Summary and conclusions

Pincer-molybdenum complexes, most notably Nishibayashi's (PNP)Mo-based and related catalysts, have demonstrated great promise for the formation of NH$_3$ from N$_2$ under mild conditions. As reported in this work, analogous (PSP)Mo complexes have been synthesized and their reactivity has been investigated, allowing us to observe intermediates and stoichiometric reactions directly relevant to this class of catalysts. In particular, our isolation of a nitride complex resulting from the cleavage of N$_2$, and the formation and characterization of the corresponding imido complexes, may offer general mechanistic insight into N$_2$ reduction pathways proceeding *via* such intermediates.

Experimentally, the reaction of **1-Cl$_3$** with an excess of reductant leads to the stable bridging-nitrogen complex **2**, while reaction with only two equivalents Na/Hg per Mo in the presence of NaI leads to facile cleavage of N$_2$ to give Mo$^{IV}$ nitride complex **1-(N)(I)**. The very strong acid [H(Et$_2$O)$_2$][BAr$^F{}_4$] protonates the nitride ligand of **1-(N)(I)**. Reaction with the moderately strong acid [LutH][OTf], which is often used for catalytic N$_2$-to-NH$_3$ conversion systems of this type, results in an equilibrium with a product that is not definitively characterized, but experimental evidence and DFT calculations indicate it to be **1-(NH)(OTf)**. [LutH]Cl, in contrast, fully reacts with **1-(N)(I)**, protonating the nitride ligand and adding chloride to the Mo center to give the fully characterized product **1-(NH)(I)(Cl)**. In the presence of additional [LutH]Cl, this Mo$^{IV}$ imide complex can then be reduced with Cp*$_2$Co resulting in the formation of NH$_3$ and returning Mo$^{III}$ complex **1-Cl$_3$**. With the relatively weak reducing agent Cp$_2$Co (Scheme 7) this reaction appears to reach equilibrium, and if base is added the reverse reaction is observed.

Results from DFT calculations are consistent with and shed light on various experimental observations, and their implications appear to apply to the (PNP)Mo analogs as well. Cleavage of N$_2$ by the reduced Mo$^{I}$ fragment to give the nitride complex **1-(N)(I)** is calculated to be kinetically facile and thermodynamically favorable, in accord with experimental results and well precedented by calculations on other (pincer)Mo systems including (PNP)Mo and (PPP)Mo.

Conversion of nitride **1-(N)(I)** to ammonia has been studied in depth. The N–H BDFE of the corresponding imide **1-(NH)(I)**, as in the case of other Mo$^{IV}$/Mo$^{III}$ nitride/imide couples, is particularly low, and its formation is intrinsically the least favorable of the three N–H bond formations leading to

ammonia. Accordingly, H-atom transfer reagents such as TEMPO-H and $CpCr(CO)_3H$ do not undergo reaction with **1-(N)(I)**. Nor does **1-(N)(I)** undergo reduction by $Cp^*_2Co$. However, in agreement with experiment, protonation of the nitride ligand of **1-(N)(I)** by [LutH]Cl, in combination with addition of the chloride anion at the trans position to yield **1-(NH)(I)(Cl)**, is computed to be kinetically facile and thermodynamically favorable.

Thus a key conclusion of this work is that protonation of the nitride, assisted by anion coordination to $Mo^{IV}$, allows a pathway for nitride-to-ammonia conversion in which "formation of the first N–H bond" is circumvented. While N-protonation by definition results in formation of an N–H bond, it is, importantly, not the unfavorable HAT or PCET that corresponds to the low N–H BDFE of (PSP)Mo(X)(N–H).

Following protonation of the nitride, HAT or PCET to the imide ligand, to yield amide, is calculated to be thermodynamically more favorable, by *ca.* 15 kcal $mol^{-1}$, than HAT or PCET to the nitride. This is the case whether or not the protonation is accompanied by anion coordination. Formation of this second N–H bond is calculated to proceed *via* a second protonation, followed by reduction (electron-transfer). Note than an initial reduction of the imide is necessarily unfavorable, since protonation followed by reduction would comprise a PCET to the nitride, and formation of the very low-BDFE "first" N–H bond. Thus the conventionally proposed pathway[35–37,57,58] of sequential HAT/PCET to the $Mo^{IV}$ nitride is not favorable, at least under conditions where reagents or potentials do not comprise a highly energy-inefficient system (*e.g.* very strong acids and reductants or very high overpotentials).

A final protonation by [LutH]X to give $[\mathbf{1\text{-}(NH_3)X_2}^+]X^-$, is calculated to be kinetically facile and very exergonic. Thermodynamically, the overall reaction of **1-(NH)X$_2$** with $Cp^*_2Co$ and [LutH]X to yield this ammonia complex is calculated to be only slightly exergonic; this is consistent with the experiments indicating that the reaction of **1-(NH)(I)(Cl)** with $Cp_2Co$ and [LutH]Cl, to give $NH_3$ and $Cp_2Co^+$, is reversible.

Alternative pathways subsequent to the initial protonation of **1-(N)X** certainly cannot be ruled out. Concerted PCET to **1-(NH)X$_2$** or **1-(NH)X$^+$** must be considered. However, the calculations – consistent with all relevant experimental observations – strongly indicate that net addition of H$^\bullet$ (PCET, concerted or otherwise) to the $Mo^{IV}$ $N_2$-cleavage product **1-(N)X**, is greatly favored by an initial protonation, accompanied by anion formation or not. Thus in the presence of sources of electron and proton sources of the type studied in this work, the lowest-energy overall sequence of $N_2$ reduction by these catalysts appears to proceed through cleavage to yield nitride, followed by addition of $H^+/X^-/H^+/e^-/H^+$, to yield coordinated $NH_3$.

We note that thioethers and pyridines are not typically regarded as closely related ligands. Therefore, the strong mechanistic similarities between the PSP and PNP Mo complexes studied in this work suggest that the conclusions drawn from this study may be generally applicable to this important class of $N_2$ reduction catalysts proceeding through $Mo^{IV}$ nitrides.

## Data availability

The authors confirm that the data supporting the findings of this study are available within the article and its ESI.†

## Author contributions

S. Man. and X. Z. conducted and analyzed the results of all synthetic and mechanistic experiments. S. Mal. and F. H. co-supervised and co-performed DFT calculations. R. N. A., L. W. G., and N. J. I. W. performed and analyzed DFT calculations. A. J. M. M. supervised electrochemical studies. Q. B. performed and analyzed electrochemical studies. T. J. E. and S. Man. collected and analyzed X-ray crystallographic data. A. S. G. supervised synthetic and mechanistic studies. S. Mal. and A. S. G. co-wrote the paper with significant contributions from S. Man., A. J. M. M., F. H. and Q. B. All authors read and approved the manuscript.

## Conflicts of interest

There are no conflicts to declare.

## Acknowledgements

This work was supported through the National Science Foundation Chemical Catalysis program under Grants No. CHE-2247259 and CHE-2247257, and through the NSF MRI Program, Award CHE-2117792. F. H. acknowledges support from the University Research Board of AUB (Award 104391). We thank Prof. Patrick Holland for helpful discussions and Prof. Jack Norton for a generous gift of $CpCr(CO)_3H$.

## Notes and references

1 V. Smil, *Enriching the Earth: Fritz Haber, Carl Bosch, and the Transformation of World Food Production*, MIT Press, Cambridge, MA, 2004.
2 J. W. Erisman, M. A. Sutton, J. Galloway, Z. Klimont and W. Winiwarter, How a century of ammonia synthesis changed the world, *Nat. Geosci.*, 2008, **1**(10), 636–639.
3 I. Rafiqul, C. Weber, B. Lehmann and A. Voss, Energy efficiency improvements in ammonia production—perspectives and uncertainties, *Energy*, 2005, **30**(13), 2487–2504, DOI: **10.1016/j.energy.2004.12.004**.
4 S. Giddey, S. P. S. Badwal, C. Munnings and M. Dolan, Ammonia as a Renewable Energy Transportation Media, *ACS Sustain. Chem. Eng.*, 2017, **5**(11), 10231–10239, DOI: **10.1021/acssuschemeng.7b02219**.
5 T. J. Del Castillo, N. B. Thompson and J. C. Peters, A Synthetic Single-Site Fe Nitrogenase: High Turnover, Freeze-Quench $^{57}$Fe Mössbauer Data, and a Hydride Resting State, *J. Am. Chem. Soc.*, 2016, **138**(16), 5341–5350, DOI: **10.1021/jacs.6b01706**.
6 A. R. Singh, B. A. Rohr, J. A. Schwalbe, M. Cargnello, K. Chan, T. F. Jaramillo, I. Chorkendorff and J. K. Nørskov, Electrochemical Ammonia Synthesis—The

Selectivity Challenge, *ACS Catal.*, 2017, **7**(1), 706–709, DOI: 10.1021/acscatal.6b03035.

7 S. L. Foster, S. I. P. Bakovic, R. D. Duda, S. Maheshwari, R. D. Milton, S. D. Minteer, M. J. Janik, J. N. Renner and L. F. Greenlee, Catalysts for nitrogen reduction to ammonia, *Nat. Catal.*, 2018, **1**(7), 490–500, DOI: 10.1038/s41929-018-0092-7.

8 J. G. Chen, *et al.*, Beyond fossil fuel-driven nitrogen transformations, *Science*, 2018, **360**(6391), eaar6611, DOI: 10.1126/science.aar6611.

9 B. H. R. Suryanto, H.-L. Du, D. Wang, J. Chen, A. N. Simonov and D. R. MacFarlane, Challenges and prospects in the catalysis of electroreduction of nitrogen to ammonia, *Nat. Catal.*, 2019, **2**(4), 290–296, DOI: 10.1038/s41929-019-0252-4.

10 W. Guo, K. Zhang, Z. Liang, R. Zou and Q. Xu, Electrochemical nitrogen fixation and utilization: theories, advanced catalyst materials and system design, *Chem. Soc. Rev.*, 2019, **48**(24), 5658–5716, DOI: 10.1039/C9CS00159J.

11 G. Hochman, *et al.*, The Potential Economic Feasibility of Direct Electrochemical Nitrogen Reduction as a Route to Ammonia, *ACS Sustain. Chem. Eng.*, 2020, **8**(24), 8938–8948, DOI: 10.1021/acssuschemeng.0c01206.

12 Q. J. Bruch, G. P. Connor, N. McMillion, A. S. Goldman, F. Hasanayn, P. L. Holland and A. J. M. Miller, Considering Electrocatalytic Ammonia Synthesis via Bimetallic Dinitrogen Cleavage, *ACS Catal.*, 2020, **10**(19), 10826–10846, DOI: 10.1021/acscatal.0c02606.

13 M. J. Chalkley and J. C. Peters, Relating N-H Bond Strengths to the Overpotential for Catalytic Nitrogen Fixation, *Eur. J. Inorg. Chem.*, 2020, **2020**(15–16), 1353–1357, DOI: 10.1002/ejic.202000232.

14 M. J. Chalkley, M. W. Drover and J. C. Peters, Catalytic $N_2$-to-$NH_3$ (or -$N_2H_4$) Conversion by Well-Defined Molecular Coordination Complexes, *Chem. Rev.*, 2020, **120**(12), 5582–5636, DOI: 10.1021/acs.chemrev.9b00638.

15 D. R. MacFarlane, P. V. Cherepanov, J. Choi, B. H. R. Suryanto, R. Y. Hodgetts, J. M. Bakker, F. M. Ferrero Vallana and A. N. Simonov, A Roadmap to the Ammonia Economy, *Joule*, 2020, **4**(6), 1186–1205, DOI: 10.1016/j.joule.2020.04.004.

16 N. Morlanés, S. P. Katikaneni, S. N. Paglieri, A. Harale, B. Solami, S. M. Sarathy and J. Gascon, A technological roadmap to the ammonia energy economy: current state and missing technologies, *Chem. Eng. J.*, 2021, **408**, 127310, DOI: 10.1016/j.cej.2020.127310.

17 S. J. K. Forrest, B. Schluschaß, E. Y. Yuzik-Klimova and S. Schneider, Nitrogen Fixation via Splitting into Nitrido Complexes, *Chem. Rev.*, 2021, **121**(11), 6522–6587, DOI: 10.1021/acs.chemrev.0c00958.

18 L. Merakeb and M. Robert, Advances in molecular electrochemical activation of dinitrogen, *Curr. Opin. Electrochem.*, 2021, **29**, 100834, DOI: 10.1016/j.coelec.2021.100834.

19 D. V. Yandulov and R. R. Schrock, Catalytic Reduction of Dinitrogen to Ammonia at a Single Molybdenum Center, *Science*, 2003, **301**(5629), 76–78.

20 K. Arashiba, Y. Miyake and Y. Nishibayashi, A molybdenum complex bearing PNP-type pincer ligands leads to the catalytic reduction of dinitrogen into ammonia, *Nat. Chem.*, 2011, **3**(2), 120–125, DOI: 10.1038/nchem.906.

21 Y. Tanabe and Y. Nishibayashi, Developing more sustainable processes for ammonia synthesis, *Coord. Chem. Rev.*, 2013, **257**(17–18), 2551–2564, DOI: 10.1016/j.ccr.2013.02.010.

22 S. Kuriyama, K. Arashiba, K. Nakajima, H. Tanaka, N. Kamaru, K. Yoshizawa and Y. Nishibayashi, Catalytic formation of ammonia from molecular dinitrogen by use of dinitrogen-bridged dimolybdenum-dinitrogen complexes bearing PNP-pincer ligands: remarkable effect of substituent at PNP-pincer ligand, *J. Am. Chem. Soc.*, 2014, **136**(27), 9719–9731, DOI: 10.1021/ja5044243.

23 H. Tanaka, K. Arashiba, S. Kuriyama, A. Sasada, K. Nakajima, K. Yoshizawa and Y. Nishibayashi, Unique behaviour of dinitrogen-bridged dimolybdenum complexes bearing pincer ligand towards catalytic formation of ammonia, *Nat. Commun.*, 2014, **5**, 3737, DOI: 10.1038/ncomms4737.

24 K. Arashiba, E. Kinoshita, S. Kuriyama, A. Eizawa, K. Nakajima, H. Tanaka, K. Yoshizawa and Y. Nishibayashi, Catalytic Reduction of Dinitrogen to Ammonia by Use of Molybdenum–Nitride Complexes Bearing a Tridentate Triphosphine as Catalysts, *J. Am. Chem. Soc.*, 2015, **137**(17), 5666–5669, DOI: 10.1021/jacs.5b02579.

25 Y. Nishibayashi, Recent Progress in Transition-Metal-Catalyzed Reduction of Molecular Dinitrogen under Ambient Reaction Conditions, *Inorg. Chem.*, 2015, **54**(19), 9234–9247, DOI: 10.1021/acs.inorgchem.5b00881.

26 H. Tanaka, Y. Nishibayashi and K. Yoshizawa, Interplay between Theory and Experiment for Ammonia Synthesis Catalyzed by Transition Metal Complexes, *Acc. Chem. Res.*, 2016, **49**(5), 987–995, DOI: 10.1021/acs.accounts.6b00033.

27 A. Eizawa, K. Arashiba, H. Tanaka, S. Kuriyama, Y. Matsuo, K. Nakajima, K. Yoshizawa and Y. Nishibayashi, Remarkable catalytic activity of dinitrogen-bridged dimolybdenum complexes bearing NHC-based PCP-pincer ligands toward nitrogen fixation, *Nat. Commun.*, 2017, **8**, 14874, DOI: 10.1038/ncomms14874.

28 K. Arashiba, A. Eizawa, H. Tanaka, K. Nakajima, K. Yoshizawa and Y. Nishibayashi, Catalytic Nitrogen Fixation via Direct Cleavage of Nitrogen–Nitrogen Triple Bond of Molecular Dinitrogen under Ambient Reaction Conditions, *Bull. Chem. Soc. Jpn.*, 2017, **90**(10), 1111–1118, DOI: 10.1246/bcsj.20170197.

29 A. Eizawa and Y. Nishibayashi, Catalytic Nitrogen Fixation Using Molybdenum–Dinitrogen Complexes as Catalysts, *Top. Organomet. Chem.*, 2017, **60**, 153–169, DOI: 10.1007/3418_2016_10.

30 Y. Ashida, K. Arashiba, K. Nakajima and Y. Nishibayashi, Molybdenum-catalysed ammonia production with

samarium diiodide and alcohols or water, *Nature*, 2019, **568**(7753), 536–540, DOI: 10.1038/s41586-019-1134-2.

31 T. Itabashi, I. Mori, K. Arashiba, A. Eizawa, K. Nakajima and Y. Nishibayashi, Effect of substituents on molybdenum triiodide complexes bearing PNP-type pincer ligands toward catalytic nitrogen fixation, *Dalton Trans.*, 2019, **48**(10), 3182–3186, DOI: 10.1039/C8DT04975K.

32 Y. Ashida and Y. Nishibayashi, Catalytic conversion of nitrogen molecule into ammonia using molybdenum complexes under ambient reaction conditions, *Chem. Commun.*, 2021, **57**(10), 1176–1189, DOI: 10.1039/d0cc07146c.

33 Y. Tanabe and Y. Nishibayashi, Comprehensive insights into synthetic nitrogen fixation assisted by molecular catalysts under ambient or mild conditions, *Chem. Soc. Rev.*, 2021, **50**(8), 5201–5242, DOI: 10.1039/D0CS01341B.

34 Y. Tanabe and Y. Nishibayashi, Recent advances in catalytic nitrogen fixation using transition metal-dinitrogen complexes under mild reaction conditions, *Coord. Chem. Rev.*, 2022, **472**, 214783, DOI: 10.1016/j.ccr.2022.214783.

35 Y. Ashida, T. Mizushima, K. Arashiba, A. Egi, H. Tanaka, K. Yoshizawa and Y. Nishibayashi, Catalytic production of ammonia from dinitrogen employing molybdenum complexes bearing N-heterocyclic carbene-based PCP-type pincer ligands, *Nat. Synth.*, 2023, **2**(7), 635–644, DOI: 10.1038/s44160-023-00292-9.

36 T. Mitsumoto, Y. Ashida, K. Arashiba, S. Kuriyama, A. Egi, H. Tanaka, K. Yoshizawa and Y. Nishibayashi, Catalytic Activity of Molybdenum Complexes Bearing PNP-Type Pincer Ligand toward Ammonia Formation, *Angew. Chem., Int. Ed.*, 2023, **62**(43), e202306631, DOI: 10.1002/anie.202306631.

37 Y. Tanabe and Y. Nishibayashi, Catalytic Nitrogen Fixation Using Well-Defined Molecular Catalysts under Ambient or Mild Reaction Conditions, *Angew. Chem., Int. Ed.*, 2024, **63**(33), e202406404, DOI: 10.1002/anie.202406404.

38 T. J. Hebden, R. R. Schrock, M. K. Takase and P. Muller, Cleavage of dinitrogen to yield a (t-BuPOCOP) molybdenum(IV) nitride, *Chem. Commun.*, 2012, **48**(13), 1851–1853, DOI: 10.1039/C2CC17634C.

39 I. Klopsch, M. Finger, C. Würtele, B. Milde, D. B. Werz and S. Schneider, Dinitrogen Splitting and Functionalization in the Coordination Sphere of Rhenium, *J. Am. Chem. Soc.*, 2014, **136**(19), 6881–6883, DOI: 10.1021/ja502759d.

40 Q. Liao, A. Cavaillé, N. Saffon-Merceron and N. Mézailles, Direct Synthesis of Silylamine from $N_2$ and a Silane: Mediated by a Tridentate Phosphine Molybdenum Fragment, *Angew. Chem., Int. Ed.*, 2016, **55**(37), 11212–11216, DOI: 10.1002/anie.201604812.

41 G. A. Silantyev, M. Förster, B. Schluschaß, J. Abbenseth, C. Würtele, C. Volkmann, M. C. Holthausen and S. Schneider, Dinitrogen Splitting Coupled to Protonation, *Angew. Chem., Int. Ed.*, 2017, **56**(21), 5872–5876, DOI: 10.1002/anie.201701504.

42 B. M. Lindley, R. S. van Alten, M. Finger, F. Schendzielorz, C. Würtele, A. J. M. Miller, I. Siewert and S. Schneider, Mechanism of Chemical and Electrochemical $N_2$ Splitting by a Rhenium Pincer Complex, *J. Am. Chem. Soc.*, 2018, **140**(25), 7922–7935, DOI: 10.1021/jacs.8b03755.

43 M. F. Espada, S. Bennaamane, Q. Liao, N. Saffon-Merceron, S. Massou, E. Clot, N. Nebra, M. Fustier-Boutignon and N. Mezailles, Room-Temperature Functionalization of $N_2$ to Borylamine at a Molybdenum Complex, *Angew. Chem., Int. Ed.*, 2018, **57**(39), 12865–12868, DOI: 10.1002/anie.201805915.

44 A. Eizawa, K. Arashiba, A. Egi, H. Tanaka, K. Nakajima, K. Yoshizawa and Y. Nishibayashi, Catalytic Reactivity of Molybdenum–Trihalide Complexes Bearing PCP-Type Pincer Ligands, *Chem.–Asian J.*, 2019, **14**(12), 2091–2096, DOI: 10.1002/asia.201900496.

45 Y. Ashida, S. Kondo, K. Arashiba, T. Kikuchi, K. Nakajima, S. Kakimoto and Y. Nishibayashi, A Practical Synthesis of Ammonia from Nitrogen Gas, Samarium Diiodide and Water Catalyzed by a Molybdenum-PCP Pincer Complex, *Synthesis*, 2019, **51**(20), 3792–3795, DOI: 10.1055/s-0039-1690151.

46 A. Egi, H. Tanaka, A. Konomi, Y. Nishibayashi and K. Yoshizawa, Nitrogen Fixation Catalyzed by Dinitrogen-Bridged Dimolybdenum Complexes Bearing PCP- and PNP-Type Pincer Ligands: A Shortcut Pathway Deduced from Free Energy Profiles, *Eur. J. Inorg. Chem.*, 2020, **2020**(15–16), 1490–1498, DOI: 10.1002/ejic.201901160.

47 J. Y. Song, Q. Liao, X. Hong, L. Jin and N. Mezailles, Conversion of Dinitrogen into Nitrile: Cross-Metathesis of $N_2$-Derived Molybdenum Nitride with Alkynes, *Angew. Chem., Int. Ed.*, 2021, **60**(22), 12242–12247, DOI: 10.1002/anie.202015183.

48 P. Garrido-Barros, J. Derosa, M. J. Chalkley and J. C. Peters, Tandem electrocatalytic $N_2$ fixation via proton-coupled electron transfer, *Nature*, 2022, **609**(7925), 71–76, DOI: 10.1038/s41586-022-05011-6.

49 Y. Ashida, Y. Onozuka, K. Arashiba, A. Konomi, H. Tanaka, S. Kuriyama, Y. Yamazaki, K. Yoshizawa and Y. Nishibayashi, Catalytic nitrogen fixation using visible light energy, *Nat. Commun.*, 2022, **13**(1), 7263, DOI: 10.1038/s41467-022-34984-1.

50 T. Itabashi, K. Arashiba, A. Egi, H. Tanaka, K. Sugiyama, S. Suginome, S. Kuriyama, K. Yoshizawa and Y. Nishibayashi, Direct synthesis of cyanate anion from dinitrogen catalysed by molybdenum complexes bearing pincer-type ligand, *Nat. Commun.*, 2022, **13**(1), 6161, DOI: 10.1038/s41467-022-33809-5.

51 T. Itabashi, K. Arashiba, S. Kuriyama and Y. Nishibayashi, Reactivity of molybdenum-nitride complex bearing pyridine-based PNP-type pincer ligand toward carbon-centered electrophiles, *Dalton Trans.*, 2022, **51**(5), 1946–1954, DOI: 10.1039/d1dt03952k.

52 L. Merakeb, S. Bennaamane, J. De Freitas, E. Clot, N. Mezailles and M. Robert, Molecular Electrochemical Reductive Splitting of Dinitrogen with a Molybdenum Complex, *Angew. Chem., Int. Ed.*, 2022, **61**(40), e202209899, DOI: 10.1002/anie.202209899.

53 A. Coffinet, D. Specklin, Q. Le De, S. Bennaamane, L. Munoz, L. Vendier, E. Clot, N. Mezailles and

A. Simonneau, Assessing Combinations of $B(C_6F_5)_3$ and $N_2$-Derived Molybdenum Nitrido Complexes for Heterolytic Bond Activation, *Chem.–Eur. J.*, 2023, **29**(26), e202203774, DOI: **10.1002/chem.202203774**.

54 A. F. Ibrahim, P. Garrido-Barros and J. C. Peters, Electrocatalytic Nitrogen Reduction on a Molybdenum Complex Bearing a PNP Pincer Ligand, *ACS Catal.*, 2023, **13**(1), 72–78, DOI: **10.1021/acscatal.2c04769**.

55 N. Ostermann, N. Rotthowe, A. C. Stückl and I. Siewert, (Electro)chemical $N_2$ Splitting by a Molybdenum Complex with an Anionic PNP Pincer-Type Ligand, *ACS Org. Inorg. Au*, 2024, **4**(3), 329–337, DOI: **10.1021/acsorginorgau.3c00056**.

56 S. Malakar, S. Mandal, X. Zhou, Q. Bruch, R. Allen, L. Giordano, N. Walker; T. Emge, F. Hasanayn, A. Miller and A. Goldman, Mechanistic Insights into Key Steps of Dinitrogen Reduction to Ammonia with Pincer ligated Mo Complexes: Case Study of Easily Reduced PSP Mo Complexes, *ChemRxiv*, 2024, preprint, DOI: **10.26434/chemrxiv-2024-2v9z2**.

57 A. Egi, H. Tanaka, T. Nakamura, K. Arashiba, Y. Nishibayashi and K. Yoshizawa, Computational screening of PCP-type pincer ligands for Mo-catalyzed nitrogen fixation, *Bull. Chem. Soc. Jpn.*, 2024, **97**(5), uoae041, DOI: **10.1093/bulcsj/uoae041**.

58 Y. Yamazaki, K. Nakaya and Y. Nishibayashi, Synthesis of Molybdenum Complexes Bearing Pyridine-Based PNP-Type Pincer Ligands with Pendent Pyridyl Unit and Their Catalytic Activity for Ammonia Formation, *Organometallics*, 2024, **43**(21), 2747–2754, DOI: **10.1021/acs.organomet.4c00290**.

59 M. J. Bezdek, I. Pappas and P. J. Chirik, Determining and Understanding N-H Bond Strengths in Synthetic Nitrogen Fixation Cycles, *Top. Organomet. Chem.*, 2017, **60**, 1–21, DOI: **10.1007/3418_2016_8**.

60 S. Kim, Y. Park, J. Kim, T. P. Pabst and P. J. Chirik, Ammonia synthesis by photocatalytic hydrogenation of a $N_2$-derived molybdenum nitride, *Nat. Synth.*, 2022, **1**(4), 297–303, DOI: **10.1038/s44160-022-00044-1**.

61 Chirik and co-workers have likewise calculated that for sequential addition of H atoms to the Mo(IV) nitride $[(depe)_2Mo{\equiv}N][BArF^4]$ (depe = 1,2-bis(diethylphosphino) ethane) to give $NH_3$, the first N–H BDFE is significantly weaker than the second and third (with an even more pronounced difference than found in this work for (PNP) MoX and (PSP)MoX nitrides); ref. 61.

62 X. Zhou, S. Malakar, T. Zhou, S. Murugesan, C. Huang, T. J. Emge, K. Krogh-Jespersen and A. S. Goldman, Catalytic Alkane Transfer Dehydrogenation by PSP-Pincer-Ligated Ruthenium. Deactivation of an Extremely Reactive Fragment by Formation of Allyl Hydride Complexes, *ACS Catal.*, 2019, **9**(5), 4072–4083, DOI: **10.1021/acscatal.8b05172**.

63 L. S. Yamout, M. Ataya, F. Hasanayn, P. L. Holland, A. J. M. Miller and A. S. Goldman, Understanding Terminal versus Bridging End-on $N_2$ Coordination in Transition Metal Complexes, *J. Am. Chem. Soc.*, 2021, **143**(26), 9744–9757, DOI: **10.1021/jacs.1c01146**.

64 Q. Liao, N. Saffon-Merceron and N. Mezailles, $N_2$ Reduction into Silylamine at Tridentate Phosphine/Mo Center: Catalysis and Mechanistic Study, *ACS Catal.*, 2015, **5**(11), 6902–6906, DOI: **10.1021/acscatal.5b01626**.

65 S. Kuriyama, K. Arashiba, K. Nakajima, H. Tanaka, K. Yoshizawa and Y. Nishibayashi, Azaferrocene-Based PNP-Type Pincer Ligand: Synthesis of Molybdenum, Chromium, and Iron Complexes and Reactivity toward Nitrogen Fixation, *Eur. J. Inorg. Chem.*, 2016, **2016**(30), 4856–4861, DOI: **10.1002/ejic.201601051**.

66 Q. J. Bruch, S. Malakar, A. S. Goldman and A. J. M. Miller, Mechanisms of Electrochemical $N_2$ Splitting by a Molybdenum Pincer Complex, *Inorg. Chem.*, 2022, **61**(4), 2307–2318, DOI: **10.1021/acs.inorgchem.1c03698**.

67 F. Hasanayn, P. L. Holland, A. S. Goldman and A. J. M. Miller, Lewis Structures and the Bonding Classification of End-on Bridging Dinitrogen Transition Metal Complexes, *J. Am. Chem. Soc.*, 2023, **145**(8), 4326–4342, DOI: **10.1021/jacs.2c12243**.

68 In marked contrast with the reaction conducted in the presence of added $I^-$, in the absence of added $I^-$ a complex mixture of products was observed by $^{31}P$ and $^1H$ NMR spectroscopy, including the "over-reduced" $N_2$-bridged Mo(0) complex (**2**) as well as some remaining Mo(III) **1-Cl$_3$**.

69 A. Katayama, T. Ohta, Y. Wasada-Tsutsui, T. Inomata, T. Ozawa, T. Ogura and H. Masuda, Dinitrogen-Molybdenum Complex Induces Dinitrogen Cleavage by One-Electron Oxidation, *Angew. Chem., Int. Ed.*, 2019, **58**(33), 11279–11284, DOI: **10.1002/anie.201905299**.

70 G. Zhang, T. Liu, J. Song, Y. Quan, L. Jin, M. Si and Q. Liao, $N_2$ Cleavage on $d^4/d^4$ Molybdenum Centers and Its Further Conversion into Iminophosphorane under Mild Conditions, *J. Am. Chem. Soc.*, 2022, **144**(6), 2444–2449, DOI: **10.1021/jacs.1c11134**.

71 Y. Kani, T. Takayama, T. Sekine and H. Kudo, Crystal structures of nitridotechnetium(V) complexes of amine oximes differing in carbon chain lengths, *J. Chem. Soc., Dalton Trans.*, 1999, (2), 209–214, DOI: **10.1039/A806245E**.

72 J. E. Weber, F. Hasanayn, M. Fataftah, B. Q. Mercado, R. H. Crabtree and P. L. Holland, Electronic and Spin-State Effects on Dinitrogen Splitting to Nitrides in a Rhenium Pincer System, *Inorg. Chem.*, 2021, **60**(9), 6115–6124, DOI: **10.1021/acs.inorgchem.0c03778**.

73 C. E. Laplaza, M. J. A. Johnson, J. C. Peters, A. L. Odom, E. Kim, C. C. Cummins, G. N. George and I. J. Pickering, Dinitrogen Cleavage by Three-Coordinate Molybdenum(III) Complexes: Mechanistic and Structural Data, *J. Am. Chem. Soc.*, 1996, **118**(36), 8623–8638, DOI: **10.1021/ja960574x**.

74 I. Klopsch, E. Y. Yuzik-Klimova and S. Schneider, in *Nitrogen Fixation*, ed. Y. Nishibayashi, Springer International Publishing, Cham, 2017, pp. 71–112.

75 B. Lindley, A. J. Miller and S. Schneider, Probing the mechanism of dinitrogen cleavage using electrochemical

methods, in *Abstracts, Southwest Regional and Rocky Mountain Regional Meeting of the American Chemical Society*, El Paso, TX, United States, November, 2020.

76 R. S. van Alten, F. Waetjen, S. Demeshko, A. J. M. Miller, C. Wuertele, I. Siewert and S. Schneider, (Electro-) chemical Splitting of Dinitrogen with a Rhenium Pincer Complex, *Eur. J. Inorg. Chem.*, 2020, **2020**(15–16), 1402–1410, DOI: 10.1002/ejic.201901278.

77 R. G. Agarwal, *et al.*, Free Energies of Proton-Coupled Electron Transfer Reagents and Their Applications, *Chem. Rev.*, 2022, **122**(1), 1–49, DOI: 10.1021/acs.chemrev.1c00521.

78 M. Brookhart, B. Grant and A. F. Volpe, [(3,5-$(CF_3)_2C_6H_3)_4B]^-[H(OEt_2)_2]^+$: a convenient reagent for generation and stabilization of cationic, highly electrophilic organometallic complexes, *Organometallics*, 1992, **11**(11), 3920–3922, DOI: 10.1021/om00059a071.

79 D. V. Yandulov, R. R. Schrock, A. L. Rheingold, C. Ceccarelli and W. M. Davis, Synthesis and reactions of molybdenum triamidoamine complexes containing hexaisopropylterphenyl substituents, *Inorg. Chem.*, 2003, **42**(3), 796–813, DOI: 10.1021/ic020505l.

80 In the absence of added [LutH]Cl, TEMPO-H (8.0 equiv.) was added to isolated (PSP)Mo(NH)(I)Cl (0.096 mmol) in THF. After 24 h at room temperature, volatiles were vacuum-transferred to a flask with HCl in diethyl ether. Ammonium chloride was only found in the receiving flask, in 41% yield. (See ESI†). (The low yield of $NH_4^+$ is attributed at least in part to some loss of $NH_3$ during vacuum transfer).

81 For a closely related example of an oxidative reaction of a pincer-Re complex with ammonia to yield a nitride complex, see: G. P. Connor, D. Delony, J. E. Weber, B. Q. Mercado, J. B. Curley, S. Schneider, J. M. Mayer and P. L. Holland, Facile conversion of ammonia to a nitride in a rhenium system that cleaves dinitrogen, *Chem. Sci.*, 2022, **13**(14), 4010–4018, DOI: 10.1039/D1SC04503B.

82 M. J. Frisch, *et al.*, *Gaussian 16, Revision A.03*, Gaussian, Inc., Wallingford, CT, 2016.

83 H. S. Yu, X. He, S. L. Li and D. G. Truhlar, MN15: a Kohn–Sham global-hybrid exchange-correlation density functional with broad accuracy for multi-reference and single-reference systems and noncovalent interactions, *Chem. Sci.*, 2016, **7**(8), 5032–5051, DOI: 10.1039/C6SC00705H.

84 M. M. Francl, W. J. Pietro, W. J. Hehre, J. S. Binkley, M. S. Gordon, D. J. DeFrees and J. A. Pople, Self-consistent molecular orbital methods XXIII A polarization-type basis set for second-row elements, *J. Chem. Phys.*, 1982, **77**(7), 3654–3665, DOI: 10.1063/1.444267.

85 M. S. Gordon, J. S. Binkley, J. A. Pople, W. J. Pietro and W. J. Hehre, Self-consistent molecular-orbital methods. 22. Small split-valence basis sets for second-row elements, *J. Am. Chem. Soc.*, 1982, **104**(10), 2797–2803, DOI: 10.1021/ja00374a017.

86 D. Andrae, U. Haeussermann, M. Dolg, H. Stoll and H. Preuss, Energy-adjusted ab initio pseudopotentials for the second and third row transition elements, *Theor. Chim. Acta*, 1990, **77**(2), 123–141, DOI: 10.1007/BF01114537.

87 K. A. Peterson, D. Figgen, E. Goll, H. Stoll and M. Dolg, Systematically convergent basis sets with relativistic pseudopotentials. II. Small-core pseudopotentials and correlation consistent basis sets for the post-d group 16–18 elements, *J. Chem. Phys.*, 2003, **119**(21), 11113–11123, DOI: 10.1063/1.1622924.

88 D. Rappoport and F. Furche, Property-optimized Gaussian basis sets for molecular response calculations, *J. Chem. Phys.*, 2010, **133**(13), 134105, DOI: 10.1063/1.3484283.

89 F. Weigend and R. Ahlrichs, Balanced basis sets of split valence, triple zeta valence and quadruple zeta valence quality for H to Rn: design and assessment of accuracy, *Phys. Chem. Chem. Phys.*, 2005, **7**(18), 3297–3305, DOI: 10.1039/B508541A.

90 F. Weigend, F. Furche and R. Ahlrichs, Gaussian basis sets of quadruple zeta valence quality for atoms H–Kr, *J. Chem. Phys.*, 2003, **119**(24), 12753–12762, DOI: 10.1063/1.1627293.

91 A. V. Marenich, C. J. Cramer and D. G. Truhlar, Universal Solvation Model Based on Solute Electron Density and on a Continuum Model of the Solvent Defined by the Bulk Dielectric Constant and Atomic Surface Tensions, *J. Phys. Chem. B*, 2009, **113**(18), 6378–6396, DOI: 10.1021/jp810292n.

92 D. Bezier, C. Guan, K. Krogh-Jespersen, A. S. Goldman and M. Brookhart, Experimental and Computational Study of Alkane Dehydrogenation Catalyzed by a Carbazolide-based Rhodium PNP Pincer Complex, *Chem. Sci.*, 2016, **7**(4), 2579–2586, DOI: 10.1039/C5SC04794C.

93 B. Auer, L. E. Fernandez and S. Hammes-Schiffer, Theoretical Analysis of Proton Relays in Electrochemical Proton-Coupled Electron Transfer, *J. Am. Chem. Soc.*, 2011, **133**(21), 8282–8292, DOI: 10.1021/ja201560v.

94 K. Arashiba, H. Tanaka, K. Yoshizawa and Y. Nishibayashi, Cycling between Molybdenum-Dinitrogen and -Nitride Complexes to Support the Reaction Pathway for Catalytic Formation of Ammonia from Dinitrogen, *Chem.–Eur. J.*, 2020, **26**(59), 13383–13389, DOI: 10.1002/chem.202002200.

95 A. Katayama and H. Masuda, in *Redox-based Catalytic Chemistry of Transition Metal Complexes*, ed. T. Kojima, Royal Society of Chemistry, 2024, vol. 2, pp. 198–230.

96 T. Wang and F. Abild-Pedersen, Achieving industrial ammonia synthesis rates at near-ambient conditions through modified scaling relations on a confined dual site, *Proc. Natl. Acad. Sci. U. S. A.*, 2021, **118**(30), e2106527118, DOI: 10.1073/pnas.2106527118.

97 C. J. M. van der Ham, M. T. M. Koper and D. G. H. Hetterscheid, Challenges in reduction of dinitrogen by proton and electron transfer, *Chem. Soc. Rev.*, 2014, **43**(15), 5183–5191, DOI: 10.1039/C4CS00085D.

98 S. Wang, F. Ichihara, H. Pang, H. Chen and J. Ye, Nitrogen Fixation Reaction Derived from Nanostructured Catalytic Materials, *Adv. Funct. Mater.*, 2018, **28**(50), 1803309, DOI: 10.1002/adfm.201803309.

99 M. Shao, *et al.*, Efficient nitrogen fixation to ammonia on MXenes, *Phys. Chem. Chem. Phys.*, 2018, **20**(21), 14504–14512, DOI: **10.1039/C8CP01396A**.

100 Y. Liu, Y. Su, X. Quan, X. Fan, S. Chen, H. Yu, H. Zhao, Y. Zhang and J. Zhao, Facile Ammonia Synthesis from Electrocatalytic $N_2$ Reduction under Ambient Conditions on N-Doped Porous Carbon, *ACS Catal.*, 2018, **8**(2), 1186–1191, DOI: **10.1021/acscatal.7b02165**.

101 Effects of varying halides have been reported in the context of $N_2$ cleavage by pincer-rhenium halide complexes, but these have been attributed to well-demonstrated effects of the halide on reduction potentials of several species involved in these reaction: R. S. van Alten, F. Waetjen, S. Demeshko, A. J. M. Miller, C. Wuertele, I. Siewert and S. Schneider, (Electro-)chemical Splitting of Dinitrogen with a Rhenium Pincer Complex, *Eur. J. Inorg. Chem.*, 2020, **2020**(15–16), 1402–1410, DOI: **10.1002/ejic.201901278**.

102 J. Chatt, A. J. Pearman and R. L. Richards, The reduction of mono-coordinated molecular nitrogen to ammonia in a protic environment, *Nature*, 1975, **253**, 39–40, DOI: **10.1038/253039b0**.

103 J. Chatt, J. R. Dilworth and R. L. Richards, Recent advances in the chemistry of nitrogen fixation, *Chem. Rev.*, 1978, **78**(6), 589–625, DOI: **10.1021/cr60316a001**.

104 R. R. Schrock, Catalytic reduction of dinitrogen to ammonia at a single molybdenum center, *Acc. Chem. Res.*, 2005, **38**(12), 955–962, DOI: **10.1021/ar0501121**.

105 R. R. Schrock, Catalytic reduction of dinitrogen under mild conditions, *Chem. Commun.*, 2003, (19), 2389–2391, DOI: **10.1039/B307784P**.

106 D. V. Yandulov and R. R. Schrock, Studies relevant to catalytic reduction of dinitrogen to ammonia by molybdenum triamidoamine complexes, *Inorg. Chem.*, 2005, **44**(4), 1103–1117, DOI: **10.1021/ic040095w**.

107 R. R. Schrock, Catalytic reduction of dinitrogen to ammonia by molybdenum: theory versus experiment, *Angew. Chem., Int. Ed.*, 2008, **47**(30), 5512–5522, DOI: **10.1002/anie.200705246**.

108 L. A. Wickramasinghe, T. Ogawa, R. R. Schrock and P. Müller, Reduction of Dinitrogen to Ammonia Catalyzed by Molybdenum Diamido Complexes, *J. Am. Chem. Soc.*, 2017, **139**(27), 9132–9135, DOI: **10.1021/jacs.7b04800**.

109 J. S. Anderson, J. Rittle and J. C. Peters, Catalytic conversion of nitrogen to ammonia by an iron model complex, *Nature*, 2013, **501**(7465), 84–87, DOI: **10.1038/nature12435**.

110 S. E. Creutz and J. C. Peters, Catalytic reduction of $N_2$ to $NH_3$ by an Fe-$N_2$ complex featuring a C-atom anchor, *J. Am. Chem. Soc.*, 2014, **136**(3), 1105–1115, DOI: **10.1021/ja4114962**.

111 L. Jones and L. Lin, A theoretical study on the isomers of the B5TB heteroacene for improved semiconductor properties in organic electronics, *Comput. Theor. Chem.*, 2017, **1115**, 22–29, DOI: **10.1016/j.comptc.2017.05.039**.

112 E. A. Buchanan and J. Michl, Optimal arrangements of 1,3-diphenylisobenzofuran molecule pairs for fast singlet fission, *Photochem. Photobiol. Sci.*, 2019, **18**(9), 2112–2124, DOI: **10.1039/c9pp00283a**.